REPORT NO.
UCB/EERC-83/21
OCTOBER 1983

EARTHQUAKE ENGINEERING RESEARCH CENTER

MECHANICAL CHARACTERISTICS OF MATERIALS USED IN A 1/5 SCALE MODEL OF A 7-STORY REINFORCED CONCRETE TEST STRUCTURE

by

V. V. BERTERO
A. E. AKTAN
H. G. HARRIS
A. A. CHOWDHURY

Report to Sponsor:
National Science Foundation

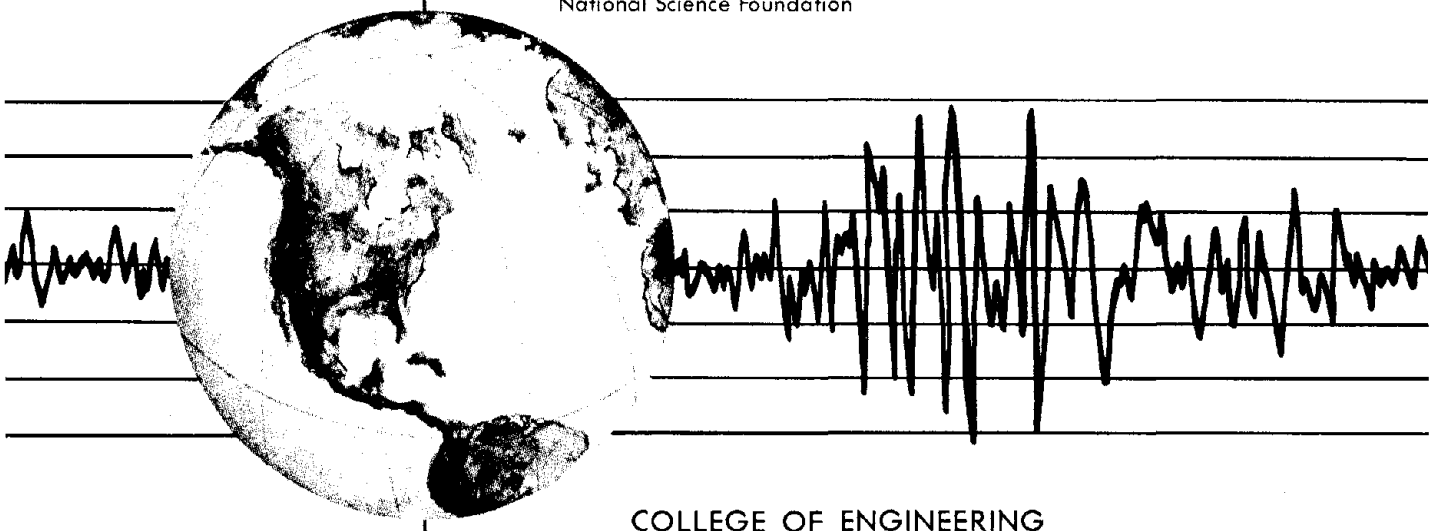

COLLEGE OF ENGINEERING

UNIVERSITY OF CALIFORNIA · Berkeley, California

For sale by the National Technical Information Service, U.S. Department of Commerce, Springfield, Virginia 22161.

See back of report for up to date listing of EERC reports.

50272-101

REPORT DOCUMENTATION PAGE	1. REPORT NO. NSF/CEE-83034	2.	3. Recipient's Accession No. PB84 193697
4. Title and Subtitle: Mechanical Characteristics of Materials used in a 1/5 Scale Model of a 7-Story Reinforced Concrete Test Structure			5. Report Date: October 1983 6.
7. Author(s): V.V. Bertero, A.E. Aktan, H.G. Harris and A.A. Chowdhury			8. Performing Organization Rept. No. UCB/EERC-83/21
9. Performing Organization Name and Address: Earthquake Engineering Research Center University of California 1301 South 46th Street Richmond, CA 94804			10. Project/Task/Work Unit No. 11. Contract(C) or Grant(G) No. (C) (G) CEE80-09478
12. Sponsoring Organization Name and Address: National Science Foundation 1800 "G" Street NW Washington, DC 20550			13. Type of Report & Period Covered 14.

15. Supplementary Notes

16. Abstract (Limit: 200 words)

One of the primary objectives of the U.S.-Japan Cooperative Research Program and the associated integrated analytical and experimental research program in progress at U.C. Berkeley is to evaluate the reliability of experimental analysis of R/C at all response limit states, utilizing a so-called true replica medium scale model, (i.e., a model which supplies simultaneous duplication of inertial, gravitational, and resisting forces).

A most serious problem encountered in the attainment of an adequate model was observed to be that of satisfying the similitude requirements for the stress-strain constitutive relations between the constituent materials of the full-scale and 1/5 scale models.

This report documents efforts undertaken to attain material similitude for the 1/5 scale model. The consequences of unavoidable distortions between the stress-strain constitutive relations and physical properties of reduced scale and full-scale model materials on the correlation of all the limit state responses of these two structural models are evaluated. It is concluded that there are still significant limitations in the state-of-the-practice of reduced scale model fabrication, particularly in micro-concrete fabrication, in which the mechanical (dynamic) characteristics and physical properties of the concrete used in the full-scale model are duplicated.

17. Document Analysis a. Descriptors

b. Identifiers/Open-Ended Terms

c. COSATI Field/Group

18. Availability Statement: Release Unlimited	19. Security Class (This Report)	21. No. of Pages 90
	20. Security Class (This Page)	22. Price

(See ANSI-Z39.18) See Instructions on Reverse OPTIONAL FORM 272 (4-77) (Formerly NTIS-35) Department of Commerce

U.S.-JAPAN COOPERATIVE EARTHQUAKE RESEARCH PROGRAM

MECHANICAL CHARACTERISTICS OF MATERIALS USED IN A 1/5 SCALE MODEL OF A 7-STORY REINFORCED CONCRETE TEST STRUCTURE

by

V. V. Bertero

Professor of Civil Engineering
University of California, Berkeley

A. E. Aktan

Associate Research Engineer
Earthquake Engineering Research Center
University of California, Berkeley

H. G. Harris

Professor of Civil Engineering
Drexel University
Philadelphia, Pennsylvania

A. A. Chowdhury

Research Assistant
Department of Civil Engineering
University of California, Berkeley

Report to Sponsor:
National Science Foundation

Report No. UCB/EERC-83/21
Earthquake Engineering Research Center
College of Engineering
University of California
Berkeley, California

October 1983

1.0

ABSTRACT

The U.S.-Japan Cooperative Research Program and the associated integrated analytical and experimental research program in progress at U.C. Berkeley incorporate the construction and testing of a 7-story full-scale R/C frame-wall structure in Japan and a true replica 1/5 scale model of this structure at U.C. Berkeley.

One of the primary objectives of the research is to evaluate the reliability of experimental analysis of R/C at all response limit states, utilizing a so-called true replica medium scale model. It is generally recognized that true dynamic models (i.e., models which supply simultaneous duplication of inertial, gravitational, and resisting forces) are practically impossible to construct. Whether an adequate model could possibly be built in R/C was, therefore, an assessment which had to be carried out first.

The most serious problem encountered in the attainment of an adequate model was observed to be that of satisfying the similitude requirements for the stress-strain constitutive relations between the constituent materials of the full-scale and 1/5 scale models.

This report documents the efforts undertaken by the researchers to attain material similitude for the 1/5 scale model. The consequences of unavoidable distortions between the stress-strain constitutive relations and physical properties of reduced scale and full-scale model materials on the correlation of all the limit state responses of these two structural models are evaluated. From this evaluation it is concluded that there are still significant limitations in the state-of-the-practice of reduced scale model fabrication, particularly in micro-concrete fabrication, in which the mechanical (dynamic) characteristics and physical properties of the concrete used in the full-scale model are duplicated.

ACKNOWLEDGEMENTS

The research reported herein was supported by the National Science Foundation, Grant Number CEE-80-09478. Any opinions, discussions, findings, conclusions and recommendations are those of the authors.

The authors are indebted to Professors R. Clough and M. Polivka for their invaluable advice in the course of this research.

The close cooperation of Professor J. K. Wight of the University of Michigan and of the Japanese researchers of the Building Research Institute at Tsukuba, Japan, in supplying information regarding the mechanical characteristics of the materials used in the construction of the full-scale test building is greatly appreciated.

Mr. D. Clyde, Development Engineer, contributed to all phases of model fabrication. His efforts and contributions in the preparation and testing of the constitutive materials are deeply appreciated.

Professor H. Krawinkler's loan of the wire knurling device from Stanford University is appreciated. The cooperation of Dr. W. G. Corley, Director of the Engineering Development Division, Construction Technology Laboratories, Portland Cement Association, in supplying some of the reinforcing bars used in the model is sincerely appreciated. The many contributions of the graduate students, development technicians and other supporting personnel associated with the research project are gratefully acknowledged. The report was edited by Susan Gardner and the illustrations were prepared by R. Steele.

TABLE OF CONTENTS

	Page
ABSTRACT	i
ACKNOWLEDGEMENTS	iii
TABLE OF CONTENTS	v
LIST OF TABLES	ix
LIST OF FIGURES	xi
1. INTRODUCTION	1
1.1 INTRODUCTORY REMARKS	1
1.2 OBJECTIVES	2
1.3 SCOPE	3
2. BASIC REQUIREMENTS OF EXPERIMENTAL ANALYSIS	5
2.1 SIMILITUDE REQUIREMENTS	5
2.1.1 Geometric Similitude	5
2.1.2 Material Response Similitude	6
2.1.3 Similitude in Weight and Reactive Mass	6
2.1.4 Similitude in Loading, Boundary and Environmental Conditions	6
2.1.5 Structural Response Analyses	7
2.1.6 Concluding Remarks	8
3. MECHANICAL CHARACTERISTICS OF REINFORCING STEEL	9
3.1 PROTOTYPE REINFORCING STEEL	9
3.2 MODEL REINFORCING STEEL	10
3.2.1 Heat Treatment of Model Reinforcement	11
3.2.2 Resulting Stress-Strain Characteristics	13
4. MECHANICAL CHARACTERISTICS OF CONCRETE	15
4.1 CONCRETE USED IN THE FULL-SCALE STRUCTURE	15
4.1.1 Concrete Mix	15

Table of Contents (cont'd) Page

4.1.2 Compressive Stress-Strain Characteristics 15

4.2 CONCRETE USED IN THE 1/5 SCALE MODEL STRUCTURE 16

4.2.1 Concrete Mix 16

4.2.2 Compressive Stress-Strain Characteristics 17

4.2.3 Tensile Strength of Model Concrete 19

4.2.4 Poisson's Ratio of Model Concrete 19

4.2.5 Shrinkage Characteristics of Model Concrete 19

4.2.6 Bond Characteristics of Model Concrete 20

5. COMPARISON OF PROTOTYPE AND MODEL MATERIAL RESPONSES 21

5.1 REINFORCEMENT 21

5.1.1 Geometric Similitude 21

5.1.2 Stress-Strain Similitude 21

5.2 CONCRETE 22

5.2.1 Compressive Stress-Strain Characteristics 22

5.2.2 Tensile Strength 23

5.2.3 Shrinkage Characteristics 23

5.2.4 Poisson's Ratio 24

5.2.5 Bond Characteristics 24

6. ASSESSMENT OF THE SUCCESS IN SATISFYING SIMILITUDE OF MATERIAL RESPONSES 26

6.1 GENERAL 26

6.2 EFFECT OF DIFFERENT MATERIAL CHARACTERISTICS ON RESPONSE . . . 26

6.3 RESPONSE PARAMETERS OF CONCRETE 27

6.3.1 Modulus of Elasticity of Concrete 27

6.3.2 Shear Modulus of Rigidity of Concrete 27

6.3.3 Poisson's Ratio 27

6.3.4 Shrinkage Coefficient 28

6.3.5 Thermal Coefficient of Expansion 28

Table of Contents (cont'd) Page

6.3.6 Strain Rate and Creep 29

6.3.7 Tensile Strength of Concrete 30

6.3.8 Compressive Strength of Concrete Under Uniaxial and Multi-Axial Stress Fields 31

6.3.9 Bond Characteristics of Concrete and Steel 31

6.3.10 Effect of Strain Gradient on Mechanical Behavior of Concrete 32

6.3.11 General Monotonic and Hysteretic Stress-Strain Response Characteristics of Concrete 32

6.4 RESPONSE PARAMETERS OF STEEL 33

6.4.1 Modulus of Elasticity 33

6.4.2 Yield Stress 33

6.4.3 Yield Plateau 33

6.4.4 Strain Hardening Modulus 34

6.4.5 Maximum Tensile Strength 34

6.4.6 Ultimate Strain 35

6.4.7 Hysteresis Characteristics 35

6.4.8 Dowel Resistance and Local Stability Characteristics . 35

7. CONCLUSIONS AND RECOMMENDATIONS 37

7.1 GENERAL CONCLUSIONS 37

7.1.1 Modelling Linear Elastic Response 37

7.1.2 Modelling Inelastic Response 38

7.1.3 Importance of Integrated Analytical and Experimental Studies 39

7.2 SPECIFIC CONCLUSIONS 39

7.2.1 Response Characteristics of Reinforcing Steel 39

7.2.2 Response Characteristics of Concrete 40

8. REFERENCES 43

TABLES 47

FIGURES 57

APPENDIX A - CONVERSION FACTORS 71

LIST OF TABLES

		Page
TABLE 1	STRESS-STRAIN CHARACTERISTICS OF PROTOTYPE STEEL	47
TABLE 2	AREA OF PROTOTYPE AND MODEL REINFORCEMENT	47
TABLE 3	CROSS-SECTIONAL AREAS OF MODEL REINFORCEMENT OBTAINED BY DIFFERENT TECHNIQUES	48
TABLE 4	STRESS-STRAIN CHARACTERISTICS OF MODEL STEEL	48
TABLE 5	CONCRETE MIXES USED IN THE PROTOTYPE	49
TABLE 6	SLUMP TESTS	49
TABLE 7	MECHANICAL CHARACTERISTICS OF PROTOTYPE CONCRETE	50
TABLE 8	CONCRETE MIX USED IN 1/5 SCALE MODEL	50
TABLE 9	MECHANICAL CHARACTERISTICS OF MODEL CONCRETE	51
TABLE 10	THE MEAN MECHANICAL CHARACTERISTICS OF THE MODEL CONCRETE FOR ALL SEVEN FLOORS	52
TABLE 11	TENSILE STRENGTH OF MODEL CONCRETE	52
TABLE 12	FORCE AND STRAIN RESPONSE CHARACTERISTICS FOR PROTOTYPE AND MODEL REINFORCEMENT	53
TABLE 13	COMPARISON OF MAIN RESPONSE PARAMETERS OF PROTOTYPE AND MODEL REINFORCEMENT	53

LIST OF FIGURES

		Page
FIG. 1	PLAN AND ELEVATION OF TEST BUILDING	57
FIG. 2	GEOMETRIC CHARACTERISTICS OF THE REINFORCING BARS USED IN THE PROTOTYPE AND MODEL	58
FIG. 3	STRESS-STRAIN RELATIONS FOR COLUMN REINFORCEMENT	59
FIG. 4	STRESS-STRAIN RELATIONS FOR BEAM REINFORCEMENT	59
FIG. 5	STRESS-STRAIN RELATIONS FOR WALL, SLAB, TIE AND STIRRUP REINFORCEMENT	60
FIG. 6	STRESS-STRAIN RELATIONS FOR THE ORIGINAL (VIRGIN) 14 GAUGE WIRE AND PCA/D2 REINFORCING BARS	60
FIG. 7	YIELD FORCE VS. 1 HOUR OVEN TEMPERATURE RELATION FOR COLUMN REINFORCEMENT	61
FIG. 8	YIELD FORCE VS. 6 HOUR OVEN TEMPERATURE RELATION FOR BEAM REINFORCEMENT	61
FIG. 9	YIELD FORCE VS. 6 HOUR OVEN TEMPERATURE RELATION FOR WALL AND SLAB REINFORCEMENT	61
FIG. 10	VIEWS OF LINDBERG HEAT TREATMENT CO. (OAKLAND) OVEN WHERE HEAT TREATMENT OF MODEL REINFORCEMENT WAS CARRIED OUT	62
FIG. 11	PHOTOGRAPH ILLUSTRATING STRAIGHTENING PROCESS FOR ANNEALED WIRE USING A LATHE AND A BENT TUBE	63
FIG. 12	EFFECT OF STRAIGHTENING WALL AND SLAB REINFORCEMENT AFTER HEAT TREATMENT	63
FIG. 13	STRESS-STRAIN RELATIONSHIP OF CONCRETE IN FIRST STORY	64
FIG. 14	STRESS-STRAIN RELATIONSHIP OF CONCRETE IN SECOND STORY	64
FIG. 15	STRESS-STRAIN RELATIONSHIP OF CONCRETE IN THIRD STORY	65
FIG. 16	STRESS-STRAIN RELATIONSHIP OF CONCRETE IN FOURTH STORY	65
FIG. 17	STRESS-STRAIN RELATIONSHIP OF CONCRETE IN FIFTH STORY	66
FIG. 18	STRESS-STRAIN RELATIONSHIP OF CONCRETE IN SIXTH STORY	66
FIG. 19	STRESS-STRAIN RELATIONSHIP OF CONCRETE IN SEVENTH STORY	67
FIG. 20	GRADATION OF GRAVEL AND TOP SAND USED IN THE MICROCONCRETE	67
FIG. 21	STRESS-STRAIN RELATIONS OF THE PROTOTYPE AND MICROCONCRETE USED TO SELECT THE MICROCONCRETE MIX FOR MODEL FABRICATION	68

FIG. 22 VARIATION OF MAXIMUM CONCRETE STRESS WITH AGE (FIRST FLOOR) . 68

FIG. 23 POISSON'S RATIO OF MODEL CONCRETE 69

FIG. 24 SHRINKAGE STRAIN OF MODEL CONCRETE WITH AGE 69

1. INTRODUCTION

1.1 INTRODUCTORY REMARKS

As part of the first joint research effort of the master program as envisioned by the Planning Group of the U.S.-Japan Cooperative Program on large scale testing [11], a seven-story R/C frame-wall earthquake resistant building has been designed, constructed and tested at the Large-Size Structures Laboratory, Building Research Institute, Tsukuba, Japan. The plan of a typical floor and the elevation of the test building prototype is shown in Figure 1. As can be seen from this figure, this test building consists of a seven-story space frame with walls. In the direction of loading and longitudinal direction there are 3 frames, each one of 3 bays. A full height shear wall is located at the mid-bay of the center frame B. In its transverse direction the test building consists of 4 frames, each one with two bays of 6 m (19.69 ft.) each and cantilevering 2 m (6.56 ft.) at each end. In the extreme transverse frames (lines 1 and 4 in Fig. 1(a)), there are full height shear walls which, as their main purpose, provide torsional resistance for the building.

From analysis of the results obtained in the analytical prediction of the responses of the prototype [5], and considering the limitations of the UC Berkeley Shaking Table, a 1/5 scale model of the prototype structure was chosen. A detailed discussion of this selection and the final design of the model structure are given in References 3 and 7.

Brief information regarding the characteristics of the materials used in the fabrication of the 1/5 scale model, as well as its design and construction, was provided in the proceedings of the third meeting of the U.S.-Japan JTCC, July 1982, Tsukuba [2,4]. Since then, pseudo-dynamic testing of the full-scale and earthquake simulator testing of the 1/5 scale models have been completed. Tests were carried out to determine the mechanical characteristics at the time of testing of the micro-concrete of the 1/5 scale model. A number of preliminary observations regarding the effects of different response characteristics of the materials on the correlations between the serviceability, damageability, and collapse limit state responses of the 1/5 scale and

full-scale structures were therefore possible.

Perhaps one of the most important objectives of the research conducted at the University of California at Berkeley on the 1/5 scale model of the structure is to evaluate the reliability of experimental analysis at all the seismic response limit states, utilizing such a medium scaled true replica model of the test structure. The most important difficulty in the attainment of a true replica model, with the same strain response history as the full-scale structure when subjected to similar seismic effects, was satisfying the similitude requirements for the response characteristics of the constituent materials of the model structure. This report was written in order to document the efforts undertaken by the researchers in order to satisfy the similitude between the material responses of the 1/5 scale and full-scale model structures. It also discusses some of the consequences of the limitations in attaining perfect similitude in the constitutive relationships of both steel and concrete, as well as their composite action, i.e., the bond characteristics, as reflected on the serviceability, damageability, and collapse limit state responses of the structure.

1.2 OBJECTIVES

The main objectives of this report are

(1) to discuss briefly the requirements to be satisfied in the selection of the model materials;

(2) to summarize the available data on the mechanical characteristics of the materials used in the construction of the full-scale model;

(3) to discuss briefly the problems encountered in the fabrication of the model materials and to present the results obtained in the determination of the mechanical characteristics of the model materials;

(4) to compare the obtained mechanical characteristics of model materials with those available from the prototype (full-scale model);

(5) to discuss the possible implications of the differences observed between the mechanical characteristics of the model and prototype structural materials.

1.3 SCOPE

To achieve the objectives in the order listed, this report consists of seven parts. After the Introduction, where the problem, objectives, and scope are defined, a brief discussion of the fundamental requirements of experimental analysis is presented in the second part. A correct simulation of all the main material response characteristics is concluded to be a necessary prerequisite to experimental analysis of nonlinear structural response. The second part of the report is concluded by discussing the efforts undertaken to identify the critical regions of the structure, and those material response parameters particularly important in attaining a correct simulation of responses of these critical regions.

The third and fourth parts of the report are devoted to discussing the mechanical characteristics of the reinforcing steel and concrete in the prototype and model. After presenting the available information regarding the characteristics of the reinforcing steel and concrete used to construct the full-scale structure, the efforts undertaken to fabricate materials for the 1/5 scale model which would satisfy the material response similitude requirements are discussed.

The fifth part of the report is devoted to a comparison of the attained linear and nonlinear response characteristics of the model reinforcement and the model micro-concrete with the corresponding characteristics of the prototype materials. While reasonably good agreement is observed between the steel responses, considerable discrepancies in the tensile strength, deformability, bond and volumetric change characteristics of the prototype and the model concrete could not be avoided.

In the sixth part of the report, the success in satisfying the similitude criteria for material responses is assessed on the basis of the data given in Chapters 2 to 5 and on the influences observed experimentally of different material response parameters on different limit state responses of the model and prototype structures. From this assessment it is concluded that the significantly higher concrete tensile strength and the higher strain rate of the model structure tested with a compressed time scale on the earthquake simulator, rather than the almost sustained load conditions imposed during the pseudo-dynamic testing of the full-scale structure,

have to result in significant differences in the damage and failure characteristics of the model and prototype structures.

General and specific conclusions and recommendations are presented in the seventh and final part of the report.

2. BASIC REQUIREMENTS OF EXPERIMENTAL ANALYSIS

2.1 SIMILITUDE REQUIREMENTS

In order to achieve a true replica model, a number of similitude requirements need to be satisfied [9]. The strains in a true replica model are expected to be identical to the corresponding strains in the prototype. For identical moduli of elasticity for model and prototype material, the forces in the model would be related to the forces in the prototype by the relation:

$$F_m = \frac{1}{L_r^2} F_p \tag{1}$$

where F_m and F_p represent the forces in the model and the prototype and L_r represents the length ratio, L_p/L_m.

In the case of inelastic and hysteretic structural response, the elastic theory of models is not sufficient. It has been suggested [8,9] that for inelastic response it is possible to obtain a correct ultimate strength model, where the strength of the model and prototype are related by expression (1), provided that a number of main similitude requirements are satisfied. In the case of reinforced concrete, some of the most important similitude requirements may be listed as follows.

2.1.1 Geometric Similitude

The first requirement pertains to the geometry. The geometry of the model structure should be proportionally identical to the geometry of the prototype structure, in accordance with the selected length ratio. This requirement, in the case of composite material, may be extended to cover the geometries of both materials, i.e., each reinforcing bar in the reinforced concrete model may also be required to be proportionally identical to the corresponding reinforcing bar in the prototype structure, including its surface deformations in addition to cross-sectional area. On the other hand, this is a very stringent requirement for many cases of experimental analysis, and the reinforcement of the prototype may be represented in a smeared manner in the model, where only the total area of reinforcement is provided with respect to

geometric similitude.

2.1.2 Material Response Similitude

This condition requires that the stress-strain constitutive relations of the constituent model materials be identical with their corresponding counterparts in the prototype. It is also required that the mechanical and chemical bond and slip characteristics also be identical between the model and the prototype constituent materials.

In general, it may not be possible to satisfy the material response similitude throughout the complete range and history of material response attained in the prototype. In fact, the state-of-the-art in the experimental determination of material stress-strain characteristics is not adequate to experimentally determine the complete stress-strain constitutive relations of a particular concrete in a general manner for all the possible combinations of states of stress, stress levels and histories. At present the only reliable test techniques available are those for the determination of the uniaxial, monotonic stress-strain responses for both concrete and reinforcing steel. Consequently, it may be possible at best to satisfy the material response similitude within this context. Even this proved to be a formidable task during the course of this research, as will be discussed later.

2.1.3 Similitude in Weight and Reactive Mass

This condition requires the specific gravity of the model materials to be higher than those of the prototype materials so that the gravity and inertial mass forces of the model may be in accordance with expression (1). Instead of using structural material with different specific gravity, the decision was made to use the same material and to satisfy this similitude requirement by using lead ballast to complement the weight of the reinforced concrete [2,7].

2.1.4 Similitude in Loading, Boundary and Environmental Conditions

Another significant similitude requirement pertains to the loading, boundary and environmental conditions. A discussion of the efforts to satisfy these conditions will be given else-

where. In general, loading of the prototype by the pseudo-dynamic scheme, while testing the model on the earthquake simulator, led to different loading strain rates and histories in the prototype and the model. Furthermore, the prototype was tested under fixed-base conditions while the model was tested under conditions simulating the rocking of the soil-foundation system due to the pitching of the table of the earthquake simulator.

The subsequent discussions will be confined to the geometric and material response similitude requirements. Since an assessment of whether a true replica model may be achieved for the reinforced concrete structure was one of the major objectives of this research, it was decided to satisfy the geometric similitude requirements as closely as possible. Consequently, each main reinforcing bar in the prototype was modeled on a one-to-one basis in the model.

2.1.5 Structural Response Analyses

While it is relatively easy to satisfy the similitude requirements for the structural materials to reproduce linear elastic behavior, serious difficulties are encountered in the simulations of the response in the inelastic range. Thus, as mentioned previously, linear elastic and nonlinear time-history analyses of the model were carried out [5] to identify the critical regions of the structure as well as those material response parameters which may be more important than others in the simulation of the inelastic structural response. The region of the wall adjacent to its base and the regions of the beams located at the interfaces of the beams with the main wall and the columns were identified as the main critical inelastic regions.

The analyses also showed that the axial and shear stresses in these critical regions were relatively low. The main wall was under a maximum axial force less than 15 percent of its balanced axial force level, and the maximum shear stress, attained only once, was less than 7.7 $\sqrt{f_c'}$ for the wall, during the response of the structure to the derived Pacoima accelerogram, with 0.4g maximum acceleration. The beams were evaluated to develop maximum shear stresses less than 2.3 $\sqrt{f_c'}$ during response. The nominal design values of 3850 psi for f_c' and 60000 psi for f_y were used in these assessments.

2.1.6 Concluding Remarks

The above results and others obtained during the analyses pointed out that the inelastic responses of the structure would be governed by the inelastic flexural responses at the base of the wall and at the beam ends. Since the associated axial and shear stresses were not judged to be critical, the uniaxial stress-strain relations of the main flexural reinforcement at the base of the wall (particularly the reinforcement at the edge members of the wall) and the main flexural reinforcement of the girders, as well as the slab reinforcement which was effective in complementing the beam reinforcement, were considered to be the most critical material responses to be incorporated in the efforts to achieve the desired similitude.

3. MECHANICAL CHARACTERISTICS OF REINFORCING STEEL

3.1 PROTOTYPE REINFORCING STEEL

Although six different sizes of reinforcing steel bars were used in the construction of the full-scale structure, only three different sizes (D10, D19, and D22) were used in the design and construction of structural components. D22 bars, with a nominal diameter of 22.2 mm (0.87 in.), were used as the main column reinforcement, including the wall edge columns. D19 bars (19.1 mm (0.75 in.) diameter) were used as the main flexural reinforcement of the girders. D10 bars (9.53 mm (0.38 in.) diameter) were used as main reinforcement in walls and slabs as well as the transverse reinforcement in beams and columns.

The D22, D19, and D10 bars were the only types of reinforcement which were modeled in the construction of the superstructure and will be considered in this report.

The geometry of the typical rebar used in Japan is shown in Figure 2. (This was not directly obtained from the Japanese researchers but from AIJ Standards for Structural Calculation of R/C Structures, Architectural Institute of Japan, 1980 [1].) The mechanical characteristics of the bars were obtained from the Japanese researchers in the form of stress-strain coupon test results, where three coupons for each type of bar were tested in the Fall of 1980. In these series of tests the Japanese researchers apparently did not obtain the complete stress-strain diagram, because only the part up to the initiation of strain hardening was reported. Therefore, further data was requested from the Japanese researchers, who, in July 1981, reported a second set of coupon test data where three coupons of each type of bar were tested and strains beyond the onset of strain hardening were recorded.

The mechanical characteristics and stress-strain responses obtained during both series of coupon tests are given in Table 1 and Figures 3-5. In these figures, the stress-strain responses of D22, D19, and D10 bars were compared against the responses of corresponding model reinforcement, which will be discussed subsequently.

It is observed in Figure 3 that there existed more than a 10 percent difference in the yield strength of D22 bars obtained from the two series of tests. No further sample tests of the reinforcement were made to the knowledge of the authors.

3.2 MODEL REINFORCING STEEL

Since it was decided to duplicate each main reinforcing bar in the full-scale structure at a one-to-one basis in the 1/5 scale model, the required nominal bar diameters were 1/5 of the diameters of D22, D19, and D10 bars, as shown in Table 2.

It was not possible to find in the market reinforcing steel bars that were geometrically similar in the scale 1/5 to the prototype deformed bars D10, D19, and D22. The required diameter of the bars would have been D2, D3.8 and D4.4. In a search through most of the research institutions which have been conducting investigations with reduced scale models of R/C structures it was found that while deformed reinforcing bars which can simulate geometrically the D10 bars were not available, the Portland Cement Association (PCA) had been using deformed bars PCA/D2 and PCA/D2.5 which geometrically could be considered as satisfying the similitude requirements illustrated in Figure 2 and Table 2. Therefore, it was decided to investigate the mechanical characteristics of these two available bars, D2 and D2.5, to see if they also satisfy the mechanical characteristics similitude requirements. Furthermore, it was decided that for simulating the D10 bars it would be necessary to deform plain wires in our laboratory at Berkeley.

The geometry of the PCA/D2.5 and PCA/D2 bars, modeling D22 and D19 bars of the full-scale structure, are observed to be somewhat different from those of the prototype bars. The deformations (ribs) of the prototype reinforcement complement the circular cross section, while the deformations of the model reinforcement were induced by removing material from the circular cross section. Consequently, the volume to effective area ratios of the prototype and model reinforcing bars were different.

Determination of the effective cross-sectional areas of the model reinforcement proved to

be difficult. One approach was to measure the weight and length of a sample. Area was obtained from:

$$Area = Weight/(Density \times Length) \quad (2)$$

where 489.61 lbs. per cubic ft. was used for the density. This approach, which may be acceptable for the prototype bar geometries as shown in Figure 2, led to an overbound in estimation of the effective cross-sectional area for the model reinforcement. The maximum and minimum net cross-sectional areas, obtained by measuring the indentations on the bars and computing the remaining area on the cross section, are compared in Table 3 to the gross area obtained from expression (2). The average values of the cross-sectional areas which were considered to represent the effective areas of the reinforcement are also included in Table 3. These areas were used to check the geometric similitude in Table 2 as well as in computing stress from force.

In order to induce the surface deformations on the plain gauge 14 wire, a knurling device made available by Professor H. Krawinkler of Stanford University [9] was used. The knurling device was originally used at Cornell University to fabricate model reinforcement [6]. The cross section and surface geometry attained after knurling the wire are shown in Figure 2. The 14 gauge plain drawn wire (diameter 0.00526 in.), from a 1021 Billet when received from the Davis Wire Company in Hayward, California, had an ultimate strength of 143 ksi and ruptured at a strain of 1.5 percent (Figure 6). Knurling this material resulted in additional cold working. The heat treating process devised to obtain the desired stress-strain characteristics from this and the other two types (PCA/D2.5 and D2) of reinforcement are discussed next.

3.2.1 Heat Treatment of Model Reinforcement

The stress-strain characteristics of all the three types of model reinforcement, PCA/D2.5 bars, PCA/D2 bars, and 1021 Billet 14 gauge drawn wire (the PCA bars were obtained as deformed and the 14 gauge wire was knurled in the laboratory) did not exhibit a definite yield point. The ultimate strength of the material ranged between 125 ksi to 140 ksi, and the ultimate strain was less than 2.0 percent, as shown in Figure 6.

In order to attain the stress-strain characteristics for the three types of reinforcement, as shown in Figures 3-5, extensive trials of heat treating processes were conducted. A number of ovens belonging to the Lindberg Heat Treatment Company in Oakland, California, as well as ovens at the Lawrence-Berkeley Laboratory of the University of California were used for this purpose.

The parameters of the heat treatment processes were: (1) the warm-up time of the oven, (2) the annealing temperature, (3) the annealing time, and (4) the cooling time of the material. All these parameters were discovered to affect the changes in the stress-strain characteristics of the virgin material. The annealing temperature affected the yield strength as well as other characteristics. The annealing time and the subsequent cooling time affected the yield plateau and hardening characteristics.

The yield force-oven time and temperature relations generated for the three types of reinforcement are given in Figures 7 to 9. These relations are observed to be quite different from each other, as affected by the metallurgical properties of the virgin material as well as any subsequent hardening imposed on the material during drawing, rolling, or deforming processes. Particularly in the case of the beam steel (Figure 8), the rate of change in yield strength with annealing temperature is observed to be considerably high. An increase of 10 degrees F in annealing temperature from 1100 degrees F to 1110 degrees F results in a 30 percent drop in yield strength.

After annealing the column bars at 1075 degrees F for one hour, it was observed that there existed a temperature gradient in the 25-foot long oven, which led to an uneven annealing along the length of the bars. Subsequent trials were, therefore, necessary to obtain the proper heat treatment cycle for these bars as the yield stress was also higher than required. A smaller 12-foot long oven, with better temperature control characteristics, was used for the subsequent heat treatment processes, as shown in Figure 10. The column bars were annealed a second time at 1100 degrees F for 1 hour and were cooled out of the oven to obtain the stress-strain characteristics given in Figure 3. The reinforcement was placed in 3-in. diameter steel

tubes for better control of the temperature distribution, with a number of thermocouples along the inside of the tubes to monitor the annealing temperature of the bars.

The beam and wall reinforcements were heat treated in the same oven inside tubes similar to the column reinforcement. The oven temperature was raised to 1120 degrees F in 5 hours and maintained for 6 hours. The material was then slowly cooled in the oven with the heat turned off. The resulting stress-strain characteristics are presented in Figures 4 and 5.

The wall steel, after knurling the 14 gauge wire obtained in spools of 2-ft. diameter from the plant, was not straight. This wire had to be guided into the tubes and retained a slight curvature after heat treating. Furthermore, its yield strength was approximately 15 percent higher than desired after heat treating. To straighten the wires after heat treating, the wires were pulled through a slowly rotating tube with a bent (Figure 11). This process affected the stress-strain characteristics as shown in Figure 12. Although the straightening was a cold-working process, it resulted in a drop of the yield stress, as shown in Figure 12.

3.2.2 Resulting Stress-Strain Characteristics

The stress-strain characteristics of the model reinforcement, as determined by a large number of coupon tests (over 24) for each type of reinforcement, are summarized in Table 4 and in Figures 3-5. The comparison of the mechanical characteristics of the prototype and model reinforcements will be discussed in subsequent sections. The response parameters of reinforcement considered in Table 4 include the modulus of elasticity, E, yield stress, f_y, the strain at onset of strain hardening, ϵ_{STH}, the strain hardening modulus at the onset of hardening, E_{STH}, the maximum tensile stress, f_u, and the ultimate strain, ϵ_u.

Since the number of tests conducted to determine the mechanical characteristics of reinforcement were adequate to obtain the variations in the main response parameters within certain confidence limits, using the tools of sample statistics, this approach was taken in constructing two bounds of stress-strain responses for each type of material, as shown in Figures 3-5. The bounds given in Table 4 were similarly evaluated for 90 percent confidence limits. Since

the reinforcing bars of the wall edge members were determined to be exceptionally critical in simulating the flexural inelastic responses of the wall in the full-scale structure, special care was exercised in their selection. Thus, the edge member reinforcement was specially selected for similitude with the corresponding material used in the prototype and should be expected to have an average yield closer to those of the prototype reinforcement than implied from Figure 3.

The comparison with the corresponding reinforcement used in the prototype will be conducted later. It is important to note, however, that the data available from the prototype included only three coupon tests for each type of reinforcement, which does not permit a thorough statistical evaluation.

4. MECHANICAL CHARACTERISTICS OF CONCRETE

4.1 CONCRETE USED IN THE FULL-SCALE STRUCTURE

Data on the properties of concrete used in the construction of the full-scale structure was obtained in April 1981 through private correspondence with Dr. J. Wight, who subsequently authored the report on the construction of the full-scale seven-story reinforced concrete test structure [12].

4.1.1 Concrete Mix

According to the available data from Japan, two different mixes were used in the construction of the structure above the foundation, with nominal design strengths of 3630 and 3840 psi. The two uppermost stories were cast with the mix with higher design strength, due to the onset of cold weather during construction. The resulting strength of the concrete in these stories, however, as will be discussed, turned out to be significantly lower than the design strength.

The concrete mixes used above the footing level of the full-scale structure are given in Table 5. The average slumps attained for concrete during the casting of each floor, as measured by a slump cone similar to the ones used in the U.S. (4 and 8 inches for upper and lower diameters, 12 inches for height) are presented in Table 6. The slumps attained for the 1/5 scale model concrete, shown in the same table, will be discussed later.

During casting, 6-in. x 12-in. cylinder samples were obtained. Some were "field" cured, similar to the structure, and some were "standard" cured in a fog room.

4.1.2 Compressive Stress-Strain Characteristics

Compression tests were carried out for 28-day strength of concrete on both standard and field cured cylinders. Stress-strain curves could not be obtained in these tests. The compressive strengths of only the field cured cylinders are given in Table 7 for the 28-day strength of prototype concrete. The strength of standard cured cylinders was approximately 20 to 40

percent higher than the strength of the corresponding field cured cylinder.

Compression tests to determine the complete stress-strain characteristics of concrete were carried out later on "field" cured specimens only. The mechanical characteristics of concrete as obtained from these tests are given in Table 7. The stress-strain curves are presented in Figures 13-19. There is no explicit information regarding the stress or strain rates in these tests. It is implied that they were conducted under strain control. Furthermore, the exact strain history is not available. It is expressed that "before a cylinder was loaded to its maximum capacity, the load was cycled three times between zero and one-third of expected maximum load" [12].

The two uppermost floors were observed to have significantly lower concrete strengths than others, as observed from Table 7 and Figures 18 and 19.

No information was available regarding beam tests for tensile strength, Poisson's ratio, shrinkage tests and shrinkage strains of concrete in structural elements for the prototype.

4.2 CONCRETE USED IN THE 1/5 SCALE MODEL STRUCTURE

4.2.1 Concrete Mix

Several trial mixes were designed and tested to obtain a micro-concrete mix which could be considered satisfactory for the purposes of material response similitude. It is acknowledged in literature that micro-concrete usually has less stiffness, larger compressive strain capacity, and larger tensile strength than regular concrete with the same compressive strength [10]. In fact, it was shown by Noor and Wijayasri [10] that adding glass beads may help to change the characteristics of micro-concrete for better stress-strain similitude with regular concrete by making it more brittle.

In the trials to determine an appropriate mix for the model, the criteria was (1) to have adequate workability, considering, particularly, the difficulty of placing and compacting concrete in the narrow and small cross sections of the model congested with reinforcement and (2) to have compressive stress-strain relations reasonably close with those obtained for the prototype, considering, particularly, the compressive strength and the secant modulus of elasticity at 45

percent of compressive strength. Other parameters of material response could not be directly incorporated in the efforts to maintain similitude, like tensile strength, volumetric change characteristics, creep characteristics, stress-strain relations under multi-axial stress fields, bond characteristics, and the effects of strain rate, environment, stress level, and history on these. The consequences of not satisfying similitude requirements in some of these response parameters will be discussed subsequently.

The mix design which was finally selected for the model is given in Table 8. Local pea gravel with a size less than 0.25 in. and local (Radum) top sand, with the gradations shown in Figure 20, were used.

The selection of this mix, resulting in an average slump of 8.1 inches (Table 6), was based on the 28-day stress-strain response of standard cured 3-in. x 6-in. cylinders, as compared to the stress-strain response of first floor concrete of the prototype (Figure 21). The prototype concrete response was obtained from field-cured, 6-in. x 12-in. cylinder samples which were 145 days old. Unfortunately, stress-strain responses of 28-day old, standard cured samples of prototype concrete were not available. This necessitated the comparison in Figure 21. Smaller cylinders were used to sample the micro-concrete in order to maintain a reasonable cylinder size to structural element size ratio in both prototype and model. As expected, it was subsequently determined that a size effect in cylinder strength existed, which will be discussed later.

4.2.2 Compressive Stress-Strain Characteristics

The correlation between the prototype and model concrete (trial) compressive stress-strain responses, as shown in Figure 21, were judged to be good, and the mix was selected based on this comparison. The necessary material for the complete model was purchased all at one time. In the concrete laboratory, the sand and gravel were prebatched and stored in airtight containers after determining the moisture content. The exact amount of water to be added to each container (barrel) was determined and marked on the container. The cement to be added to each container was weighed and prepared before casting.

The casting of the model structure was described previously [2]. In spite of the precautions and effort undertaken in order to maintain uniform concrete properties in the model, considerable variation still occurred. Furthermore, the mechanical characteristics obtained for the micro-concrete changed significantly with time, more than expected, leading to considerable discrepancy with the stress-strain relations of the prototype concrete, as will be discussed subsequently. Some of the mechanical characteristics of concrete attained for the model, and the changes in these characteristics with age, are indicated in Table 9. The average values of compressive strength, f_{cmax}, strain at maximum stress, ϵ_o, and the secant modulus of elasticity at 45 percent of compressive strength, $E_{0.45f_{cmax}}$, were compared at 28 days, 159-216 days, and 399-456 days for the seven stories of the model. The standard deviations in these quantities, $\sigma_{f_{cmax}}$, σ_{ϵ_o}, and $\sigma_{E0.45f_{cmax}}$, respectively, were also evaluated for each story, as shown in the same table. The typical stress-strain relations of the model concretes at different ages are also given in Figures 13-19. Discussion of the comparison with prototype concrete responses, included in the same figures, will be carried out later.

The most striking observations from Table 9 are the changes in model micro-concrete characteristics with age. The compressive strength of first-story concrete increased as much as 58 percent between 28 and 216 days. This is illustrated in Figure 22 and was not an expected phenomenon. The strength increase reported for the first-story concrete of the full-scale structure was 14 percent, as shown in Figure 22.

The strain of model concrete at maximum stress is also observed to increase with age, approximately 20 percent for first-story micro-concrete, between 28 and 208 days. The secant modulus of elasticity increased less than 10 percent between 28 and 216 days but decreased by the same amount between 216 and 456 days for the first-story micro-concrete.

The average values of f_{cmax}, ϵ_o, and $E_{0.45f_{cmax}}$ (i.e., $\bar{f}_{cmax}$, $\bar{\epsilon}_o$, and $\bar{E}_{0.45f_{cmax}}$) for the complete structure and the standard deviation (σ) in these quantities over the model structure are listed in Table 10, showing the changes in these average characteristics with age. An interesting observation is the standard deviation of concrete strength over the structure: 456 psi at 28

days, 249 psi at an average of 187 days, and 123 psi at an average of 427 days. This indicates that the variation in concrete strength decreased with the aging of concrete.

4.2.3 Tensile Strength of Model Concrete

Split cylinder (3 in. by 6 in.) and third-point loaded, 5 in. by 6 in. by 20 in. beam tests were conducted at an average age of 187 days to determine the tensile strength of concrete. Results are presented in Table 11. The average split cylinder tensile strength for the seven-stories were obtained as 747 psi with a standard deviation of 32 psi. As the function of the $\sqrt{f_c'}$, this resulted in 9.9 $\sqrt{f_c'}$, using the mean value of 5684 psi for f_c' obtained for the complete model at 190 days of age, as shown in Table 10. The beam tests (two samples for each story) yielded the same average tensile strength with a standard deviation of 70 psi. This was not expected as the modulus of rupture beams usually yield a higher tensile strength than split cylinder tests.

4.2.4 Poisson's Ratio of Model Concrete

The variation of Poisson's ratio with stress is drawn in Figure 23. This figure is for the model only. These curves were generated while doing compression tests on 3-in. x 6-in. cylinders. The age of the cylinders varied from 159-219 days, as indicated in Figure 22. The Poisson's ratio at stresses less than 3 ksi (54 percent of f_{cmax}) varied from 0.135 to 0.217. The overall average in this stress range was 0.15.

Poisson's ratio of the prototype concrete was not available.

4.2.5 Shrinkage Characteristics of Model Concrete

Shrinkage tests on the model concrete were done on 3-in. x 3-in. x 11-in. plain concrete prisms. These specimens were immersed under water for at least 7 days and then taken out and exposed to drying, measuring the shrinkage at certain time intervals. The shrinkage tests were done on concrete specimens of the bottom four floors, and the curves of shrinkage strain vs. age are shown in Figure 24. As can be seen from this figure, for the first floor, concrete

shrinkage strains were measured up to a concrete age of 40 days. At 7 days the shrinkage was 0.000425 in/in. At 24 days the rate of increase of the shrinkage strain dropped, and the strain became 0.0011 in/in. at 40 days. For the second floor, the initial shrinkage was higher than the first floor but then dropped down below the first floor level.

Shrinkage data for the prototype were not available.

4.2.6 Bond Characteristics of Model Concrete

The bond characteristics between model concrete and PCA/D2.5 bars used for the main column and shear wall edge member reinforcement were investigated. Concrete blocks, 3-in. x 3-in. in dimensions, were used to conduct pullout tests on bars with bonded embedment lengths of 1 in., 2 in., and 4 in.

The maximum average bond stresses attained for the 1 in. and 2 in. embedment lengths were 1838 psi and 1010 psi, respectively. The bars with the 4-in. embedment length fractured during the test before total slippage was possible.

The development length l_d for the model concrete and rebar, evaluated from the lower bound of bond stress attained for the 2-in. bonded specimens, is 2.34 in., i.e., 13.5 bar diameters. The ACI requires a minimum development length of 4.16 in. for a bar of this diameter, as obtained from $l_d \geqslant 0.0004 d_b f_y$,* where l_d is the development length, d_b is the diameter, and f_y is the yield stress.

When the experimentally obtained development length of 2.34 in. for the model reinforcement and concrete was compared with experimental data available from tests conducted on standard #6 and #8 deformed bars,** the bond characteristics of the model materials used in the columns were assessed to be somewhat better than the corresponding characteristics of the prototype materials.

---

*The other ACI expression, $l_d = 0.04 A_f f_y / \sqrt{f'_c}$, does not govern in this case.

**Eligehausen, R., Bertero, V. V., and Popov, E. P., "Analytical Model for Deformed Bar Bond Under Generalized Excitations, Tests and Analytical Model," Earthquake Engineering Research Center, report in preparation, University of California, Berkeley, 1983.

5. COMPARISON OF PROTOTYPE AND MODEL MATERIAL RESPONSES

5.1 REINFORCEMENT

5.1.1 Geometric Similitude

The geometry of surface deformations of the prototype and model reinforcement was given in Figure 2. The cross-sectional areas were compared in Table 2. An error in the area of the PCA/D2.5 bar of 9 percent is observed, limiting the attained geometric similitude. Furthermore, the deformation patterns of model reinforcement indicate better mechanical bonding characteristics, verified by pullout tests. In general, however, the geometric similitude may be considered to be reasonably satisfied between the model and prototype, both for overall element geometries as well as for individual reinforcing bar geometries.

5.1.2 Stress-Strain Similitude

The stress-strain responses of prototype and corresponding model reinforcement were presented in Figures 3-5 and in Tables 1 and 4. Considering the modulus of elasticity, E, yield force, F_y, strain at onset of strain hardening ϵ_{STH}, modulus of strain hardening at the onset of strain hardening, E_{STH}, maximum tensile strength, f_u, and ultimate strain, ϵ_u, as the important uniaxial stress-strain response parameters for reinforcing steel, they were compared in Tables 12 and 13. It is observed that the ratio of prototype and model reinforcement response parameters are close when moduli of elasticity, yield force, and maximum tensile strength and strain are considered (within 10 percent), but larger differences in length of yield plateaus ($\epsilon_{STH} - \epsilon_y$) and initial strain hardening moduli (as much as 65 percent) were attained. As discussed previously, additional efforts were undertaken in the selection of the shear wall edge member reinforcement to result in better correlation in the response parameters of this reinforcement with those of the corresponding prototype reinforcement.

5.2 CONCRETE

5.2.1 Compressive Stress-Strain Characteristics

The compressive strength of model concrete was obtained by testing 3-in. x 6-in. cylinders while 6-in. x 12-in. cylinders were used for testing prototype material. All cylinders were capped. The smaller cylinders were observed to yield 22 percent higher strength when 6-in. x 12-in. cylinders of the same concrete (three cylinders of each size, from fifth story concrete) were tested at the same age of 170 days.

The mean compressive strength of concrete attained in the first five stories of the prototype structure at an age of 98-145 days was 4096 psi. The average strength of model concrete at 159-216 days of age was 5684 psi at the commencement of testing on the earthquake simulator.

The stress-strain relations of the model were given in Figures 13-19. Considering that the characteristics of the first-story concrete would be particularly consequential in the overall responses of the structure, the strengths of prototype and model concrete at this story were 4111 psi (145 days) and 5682 psi (216 days), respectively. Adjusting model concrete strength for the 22 percent size effect, this strength becomes 4657 psi, 13 percent higher than prototype concrete. On the other hand, if the smaller cylinders are considered to yield more representative strength for the model concrete in the smaller elements of the model, the adjustment for size effect should not be incorporated.

The strain at maximum stress was 0.00218 (145 days) and 0.0035 (208 days) for the prototype and model concretes of the first story, respectively, indicating considerably higher deformability of the micro-concrete.

The secant modulus of elasticity at 45 percent of ultimate strength was 3150 ksi (145 days) and 3160 ksi (208 days) for the prototype and model concretes of the first story, i.e., very close to each other. The stress-strain relations of model concrete after attaining ultimate strength were obtained by a number of cycles of unloading and reloading under load control

and a stress rate of 2000 psi per minute. The attained spalling strain was 0.0075. The spalling strain attained for prototype concrete tested under strain control was 0.0055.

It is believed that the value of the spalling strain is quite sensitive to strain rate, strain history, and strain gradient. Thus, it is not easy to assess the significance of the above values.

It is of importance to recognize the effects of testing different sizes of cylinders in order to sample the concrete of the full-scale and 1/5 model structures. Although it is acknowledged* that the effects of size in concrete testing is not yet fully understood, maintaining a correct relationship between the sizes of the critical elements of the structure and the cylinder sample is known to be important. The question which should be answered by urgent research is: *What would be the sample size which would yield more representative stress-strain characteristics for the micro-concrete in the 1/5 scale model?* Although the authors believe that the used 3-in. by 6-in. control cylinders were adequate for the 1/5 scale model, whether or not 6-in. by 12-in. or 3-in. by 6-in. or 6/5 in. by 12/5 in. cylinders would have been more realistic requires further investigation.

5.2.2 Tensile Strength

The average tensile strengths of model and prototype concrete (first 5) stories were 747 psi and 377 psi (or 10.9 $\sqrt{f_c'}$ and 5.88 $\sqrt{f_c'}$ using the $\sqrt{f_c'}$ values in psi as described in Section 5.2.1 for the first-story concrete in the model and the prototype), respectively, indicating that the micro-concrete possessed almost twice the tensile strength of the prototype concrete. The importance of this much higher tensile strength, particularly in cracking, will be discussed later.

5.2.3 Shrinkage Characteristics

The important factors affecting shrinkage of concrete are known to be (1) water-cement ratio, (2) thickness of member, (3) aggregate content, size, and quality, (4) relative humidity and temperature. A very large shrinkage strain of 0.0011 in/in. was measured for the model

*Structural Modeling and Experimental Techniques by G. M. Sabnis, H. G. Harris, R. N. White, and M. S. Mirza, Prentice Hall, Inc., Englewood Cliffs, New Jersey, 1983.

concrete at 40 days from 3-in. x 3-in. x 11-in. plain concrete prisms (Fig. 24). Since the water-cement ratio of the model was 0.67 while it was 0.51 for the prototype, and since the gravel/sand weight ratios were 0.27 and 1.26 for the model and the prototype, respectively, the prototype concrete is expected to shrink considerably less. Unfortunately, no data on shrinkage of prototype concrete was available.

Since shrinkage is affected by the thickness of the element, the model concrete is expected to shrink more than the prototype concrete due to this parameter only.

Shrinkage, and more importantly, differential shrinkage between walls and columns of the model structure were observed to be consequential in the axial force distribution of the elements at the base of the structure [3].

5.2.4 Poisson's Ratio

The Poisson's ratio obtained from tests on the model concrete ranged from 0.13 to 0.34, depending on the age and compressive stress level (Figure 23). For compressive stresses below 0.45 f_c', the average value of Poisson's ratio was 0.176. Since the shear modulus of rigidity of concrete is related to the Poisson's ratio, and since the shear distortions of the main shear wall affected the structural response considerably in the serviceability and damageability limit states, the Poisson's ratio is an important parameter to consider in attaining similitude. No data was available on the Poisson's ratio of the prototype concrete. However, it is expected not to differ very much from the values obtained from the model.

5.2.5 Bond Characteristics

The bond characteristics of model materials were already assessed to be somewhat superior to those of the prototype material. The development length of the main column bar in the prototype, based on the ACI approximate expression ($0.04\ A_b f_y/\sqrt{f_c'}$, was 24 inches, while the corresponding model bar had a development length of 2.34 inches. The ratio of development lengths is 10.25, twice the length ratio of 5 between the prototype and the model. Consequently, the slippage of reinforcement and the deterioration of bond under reversals are

expected to be relatively smaller for the model under the same stress levels as for the prototype. In addition, the flexural hysteresis characteristics of model members as affected by pullout or bond slippage and deterioration should be expected to be superior to those of similar members in the prototype.

6. ASSESSMENT OF THE SUCCESS IN SATISFYING SIMILITUDE OF MATERIAL RESPONSES

6.1 GENERAL

It was discussed earlier that the similitude requirements derived from the theory of elastic models are not sufficient for simulating responses when it involves inelastic behavior of the structural material, particularly when post-cracking and post-yield responses of reinforced concrete are considered. It was argued, however, that if a number of similitude requirements may be satisfied, the strain history of the model may be representative of the prototype, and the response characteristics of the prototype may be estimated from the observed stiffness, strength, hysteresis and failure characteristics of the model [8,9]. The primary requirement for this is to be able to satisfy similitude between the critical response characteristics of the model and the prototype materials. In this section, discussions are provided of: (1) how different material characteristics could affect structural response and (2) whether the efforts to maintain material response similitude were successful and adequate to attain similitude of the structural responses of the model with respect to the prototype response. Some results of tests conducted on model and prototype are used as background for the discussion.

6.2 EFFECT OF DIFFERENT MATERIAL CHARACTERISTICS ON RESPONSE

In the case of the reinforced concrete frame-wall structure, different material response parameters were observed to affect different structural response characteristics, depending on the limit state of response. Due to the main characteristics of the final designed structure and of its careful detailing, analysis shows that the response is dominated by the main shear wall during all limit states. Consequently, those material response characteristics which particularly affect the structural wall response during serviceability, damageability, and collapse limit states will affect the complete structural response during the same limit states. A listing and brief discussion of the observed critical material response parameters follows.

6.3 RESPONSE PARAMETERS OF CONCRETE

6.3.1 Modulus of Elasticity of Concrete

The modulus of elasticity directly affects the uncracked flexural stiffness of all elements during the uncracked serviceability limit state responses. Tests showed that slight fluctuations in the stress level of concrete affected the fundamental frequency of the structure about 10 percent [3] at low stress levels. However, similar fluctuations in stress level affected the fundamental frequency only 5 percent when the average stress level of concrete was higher, corresponding to the full gravity stress level of the structure. Obviously the contribution of the modulus of elasticity of concrete depends on the stress level. Good correlation (almost 100 percent) was achieved between the secant moduli of elasticity of model and prototype concrete at 0.45 of ultimate strength.

6.3.2 Shear Modulus of Rigidity of Concrete

This parameter, which could not be directly incorporated in the efforts to maintain material response similitude, has to directly affect the uncracked shear flexibility of the wall, which it has been shown to contribute to (depending on the moment-to-shear ratio, axial stress, and other factors) approximately 35 percent of the total flexibility of this element at the serviceability limit state [3]. Shear modulus was observed to be dependent on the stress level in concrete. Tensile stress or small axial compressive stress resulted in a significant reduction of shear modulus of wall concrete. Very little reliable information exists regarding the variation of the concrete shear modulus of rigidity with the variation of axial force and, particularly, with micro-cracking. Thus, it is necessary to experimentally determine and investigate this parameter further.

6.3.3 Poisson's Ratio

Poisson's ratio was observed to be dependent on the stress level of concrete. However, Poisson's ratio measured from cylinder tests indicated a constant value for this parameter until at least 50 percent of the cylinder strength was attained. Had the Hookean relation between

Poisson's ratio, modulus of elasticity and modulus of rigidity in the case of isotropic material (i.e., $E/G = 2(1+\nu)$ been applicable to concrete, the modulus of rigidity could have been obtained from E and ν. It was observed, however, that the shear stiffness, and hence, the modulus of rigidity of concrete was far more influenced by the stress level of concrete than E or ν, particularly when tension or very small compressive stress were present.

6.3.4 Shrinkage Coefficient

The shrinkage of concrete affected initial precracking tensile stress in the concrete. Furthermore, differential shrinkage between different structural members at the same story was observed to affect the force distribution of these members significantly [3] to the extent that such forces were in the same order of magnitude as the gravity forces in the structure.

Shrinkage is expected to be significantly higher in the model than in the prototype since the water to cement ratio of model concrete was 31 percent higher, its aggregate content 4.7 times lower, and member thicknesses of the model 5 times smaller. The resulting effects of differential shrinkage are also expected to be higher in the model since shrinkage is higher.

The effects of shrinkage become less important after cracking occurs in the member and the shrinkage stresses are released. However, since shrinkage and differential shrinkage stresses affect the location and initiation of cracking, they also affect the post-cracking response in an indirect manner.

6.3.5 Thermal Coefficient of Expansion

This was a parameter which was observed to affect structural response similar to the shrinkage and differential shrinkage. Unfortunately, in the laboratory in which the specimen was constructed it was not possible to control the ambient temperature. Thus, the cycles of temperature during the day and night resulted in forces in the model on the same order of magnitude as the gravity forces. This parameter could not be incorporated in the efforts to maintain material response similitude.

6.3.6 Strain Rate and Creep

The stiffness and particularly the strength of concrete are known to increase with the strain rate while creep, particularly short-term creep, is known to affect the modulus of elasticity adversely. At low stress levels, this may not be a significant effect. At high load levels, however, during damageability response, the effect of creep may become quite important on the behavior of the structure, particularly if the load level is sustained for a long duration. It is believed that creep of concrete, together with strain rate effects, played a significant role in the loss of similitude between model and prototype. Due to the pseudo-dynamic testing procedure for the prototype and earthquake simulator testing of the model with a compression of the time scale by $\sqrt{5}$, the relative strain rates of prototype and model concretes were significantly different. As in the case of pseudo-dynamic testing, the full-scale model was subjected to roof-controlled displacement, and the loads applied to each floor were maintained in a constant ratio, resulting in an inverted triangular load pattern through the height of the structure. Then the prototype was under the influence of a nearly sustained load effect, which accentuated the relaxation and redistribution of stress. On the other hand, the model material was subjected to a high strain rate which did not permit an important redistribution of stress due to creep. The consequences of this and the differences in the tensile strength capacities of the concrete as well as the differences in the bond characteristics and the effect of strain gradient on the distribution and width of cracks in the model and the prototype are considered to be important. While the cracking in the lower stories of the shear wall of the prototype was closely and uniformly distributed, the cracking in the model was concentrated in the first story and, particularly, at the base. This affected the correlation in the stiffness and strength characteristics of the model and prototype as well as the damage mechanisms in the damageability limit states and the mode of failure in the collapse limit state.

The finely spaced cracking distributed throughout the first three stories of the prototype helped in the dissipation of energy through friction. Also, during hysteretic response the integrity of the panel concrete was affected due to a large number of cracks crossing each other.

The continued abrasion and deterioration of concrete along the crack surfaces resulted in a considerable portion of the energy being dissipated through shear friction, while reducing the demands on the edge member reinforcement. Meanwhile, since this mechanism could not develop in the model, most of the energy dissipation demand had to be satisfied through yielding of reinforcement of the wall edge members at the base as well as the slippage of this reinforcement from the foundation. Consequently, the initial crack patterns influenced the further development of cracking and affected the manner in which increases in demands were resisted or supplied by the structure.

The concentration of cracking at the base of the wall in the model, and the subsequent increases in demands leading to yielding and slipping of the main flexural reinforcement in this region, finally triggered a flexural failure of the wall by extensive yielding, kinking, buckling, and rupturing of this reinforcement. On the other hand, the finely spaced and distributed cracking in the prototype led to an increase in shear friction demands from the concrete at particularly the lower portions of the first story wall panel. However, the intersecting diagonal cracks that cyclically opened and closed resulted in abrading and considerable weakening of the concrete. Early crushing of the concrete and the spreading of such crushing over the entire length of the wall led to a shear-compression failure of the whole wall panel.*

6.3.7 Tensile Strength of Concrete

The tensile strength of concrete was important in defining the stress level at which cracking occurred. The average tensile strength of the model concrete was double that of the prototype concrete. The cracking moments of the beams and wall of the model, particularly when under zero or low axial compression, were very close to the yield moments. Consequently, yielding of reinforcement followed cracking immediately or after only a slight increase in the stress level. This did not permit the distribution of cracking, as it localized damage to the location of initial cracking and deterred the initiation of further cracks.

*Information on the failure mechanism of the prototype was obtained from the preliminary draft prepared by Okamoto et al of B.R.I., Japan, and included in the Proceedings of the Third U.S.-Japan JTCC at Tsukuba, Japan, July 1982.

The consequences of the higher tensile capacity of model concrete were similar to those discussed for the strain rate and creep effects. The differences in the damage distribution and failure patterns between the model and prototype were accentuated due to the higher tensile capacity of model micro-concrete.

6.3.8 Compressive Strength of Concrete Under Uniaxial and Multi-Axial Stress Fields

The similitude between the compressive strength and failure characteristics of concrete, not only under uniaxial stress, but as affected by the multi-axial stress fields, stress levels and histories were observed to be important in achieving similitude in structural responses, particularly in the collapse limit state. Since the failure in the prototype was through a multi-axial shear-compression (splitting and crushing) failure of panel concrete, the strength and failure characteristics of concrete directly affected the ultimate strength and failure mode of the prototype.

The failure of the model was through flexure at the base of the wall and, thus, was not as directly affected by the shear-compression failure characteristics of concrete, particularly due to the low axial stress level. On the other hand, the shear-friction (interlocking) capacity of concrete might have affected the post-flexural failure limit state responses of the model.

The compressive strength of concrete in the model was at least 14 percent higher than the prototype material. The failure characteristics under complex stress fields was not investigated. The higher ductility of micro-concrete, however, may be considered as an indication of higher resistance to deterioration and an extended, if not higher, shear-friction (interlocking) capacity.

6.3.9 Bond Characteristics of Concrete and Steel

These characteristics significantly affected cracking and, in particular, post-yield responses of the structure. Since bond-slip reduces the flexural stiffness, and particularly the dissipation of energy because of the resulting pinching in hysteretic behavior, a lack of similitude in the bond characteristics between model and prototype has to affect similitude in the structural damageability and collapse limit state responses.

The local bond stress-slip between micro-concrete and reinforcement of the model before total slippage (bond capacity) was determined to be superior to the corresponding prototype materials. Thus, a better hysteretic behavior should be expected for the model than for the prototype.

6.3.10 Effect of Strain Gradient on Mechanical Behavior of Concrete

Flexural strength and ductility of the small scale model increases with the strain gradient along the length of the members as well as the strain gradient across the sections of members [10]. Therefore, the strength, ductility, and energy dissipation capacity of the reduced scale model should be expected to surpass that of the prototype when all the other factors are perfectly simulated.

6.3.11 General Monotonic and Hysteretic Stress-Strain Response Characteristics of Concrete

In addition to the response characteristics of concrete, other parameters should be considered for a thorough evaluation of whether similitude between model and prototype concrete responses could be achieved. In general, the discrete parameters of material response, and particularly material failure characteristics, which were discussed so far, constitute most of the critical aspects of material behavior. For a complete assessment, however, the similitude in the general constitutive relations between all stress and strain components, under any combination and history of stresses, throughout the possible bounds of tensile and compressive stresses and strains that the material may be subjected to, should be investigated. Unfortunately, concrete defies a generalized formulation of its constitutive relations due to its extreme complexity and variability and due to the exceptionally large number of parameters which affect its response. Furthermore, the state-of-the-art in the experimental evaluation of the response parameters of concrete is not adequately advanced to reliably evaluate all the critical response parameters of this material. Consequently, it is not possible to carry out a complete assessment of the achieved similitude in the responses of model and prototype concrete.

6.4 RESPONSE PARAMETERS OF STEEL

6.4.1 Modulus of Elasticity

The modulus of elasticity affects the cracked flexural stiffness of members. Because good correlation between the moduli of elasticity of both model and prototype reinforcement (98 percent) was achieved, no significant effects can be attributed to the lack of perfect similitude of this parameter.

6.4.2 Yield Stress

This is one of the most critical material response parameters which affected the stiffness, strength, and energy dissipation characteristics and complete response history of the structure in the inelastic range. The initiation of first yield and the sequence of subsequent yielding in the structure are significantly affected by the relative yielding strengths of different critical regions, which, in turn, depend on the yield stress of reinforcement at these critical sections.

Particular emphasis was given in satisfying yield stress similitude of edge member flexural reinforcement at the base of the wall. The correlation was approximately 94 percent. Thus, no significant effect can be expected from different yielding stresses of the reinforcing steel in the model or in the prototype.

6.4.3 Yield Plateau

The length of the yield plateau is another important parameter affecting the spread of yielding at a plastic hinge and, therefore, the sequence of yielding within the structure. If the plateau is long, the spread of yielding along the inelastic region (plastic hinge) is restricted. If observed bond deterioration with increase in steel strain is neglected, propagation of yield along adjacent cross sections cannot begin before the section which yielded first can increase its strength through strain hardening.

The length of the yield plateau was observed to be one of the most difficult characteristics of steel response to simulate the model reinforcement. A correlation of 80 percent for column

and only 55 percent for beam reinforcement was attained. When the effects of the substantially longer yield plateau of model beam reinforcement were combined with the previously discussed effects of concrete tensile strength and strain rate, the overall force redistribution characteristics of model and prototype became further apart. Fortunately, the overall behavior was controlled by the inelastic behavior of the wall in the region adjacent to the foundation, and there the correlation of yielding plateau was better.

6.4.4 Strain Hardening Modulus

This parameter has to affect the post-yield responses of the structure. The higher the strain hardening modulus of steel, the more propagation of yield along a member occurs. Model reinforcement possessed considerably lower strain hardening moduli on the order of 0.30-0.60 of the hardening moduli of prototype reinforcement. Thus, the spreading of the critical region in the model should have been delayed with respect to the prototype.

6.4.5 Maximum Tensile Strength

This parameter affects the ultimate flexural capacity of very ductile flexural regions. Since the flexural capacity at the base of the wall was attained during the responses of the model, and this was the mode of failure of the wall, the importance of the maximum tensile strength of reinforcement is evident. The maximum strength of reinforcing steel, however, is strongly influenced by the strain history (kinematic hardening) as well as whether it had been subjected to buckling and kinking previously.

The maximum strength of model column reinforcement was 12 percent less than the maximum strength of prototype reinforcement as obtained from coupon tests. The post-yield strain histories of the wall edge members reinforcing bars of the base of the wall, however, were different in the model and prototype, which makes a prediction of the possible effects of this parameter on structural response similitude difficult. However, it is believed that this effect could not be larger than 12 percent.

6.4.6 Ultimate Strain

The value of this parameter was larger than 0.17. Usually this is more than is required in the response of a structure. Only in a very ductile structure can the reinforcing steel be stretched to its ultimate strain. This was the case of the model. This parameter controlled the behavior of the edge member at the base of the shear wall affecting the rotation capacity of this region. The ultimate strain of model edge member reinforcement was 11 percent larger than the strain capacity of the prototype reinforcement. On the other hand, the actual strain capacity is affected by the previous strain history, and the strain histories of model and prototype reinforcement were different. The reinforcement of the wall edge member at the base of the model ruptured, while this apparently did not occur in the prototype.

6.4.7 Hysteresis Characteristics

The hysteretic energy dissipation and hardening characteristics of steel are directly reflected on the post-yield responses of the structure. These material characteristics could not be incorporated in the efforts to achieve material response similitude.

6.4.8 Dowel Resistance and Local Stability Characteristics

In assessing the response parameters of reinforcing steel which affect structural response, so far the uniaxial stress-strain characteristics were considered. Along a cracked region the dowel resistance and buckling characteristics of the reinforcing steel are important, particularly at the ultimate limit states. These parameters could not be incorporated in the efforts to maintain similitude between model and prototype responses. To simulate dowel characteristics, it is necessary to consider the crack width and the bearing characteristics of concrete at each face of the crack and adjacent to the reinforcement, since these parameters affect the kinking behavior of the reinforcement. The kinking behavior, in turn, affects the dowel resistance characteristics.

The cross-sectional shapes of the model and the prototype reinforcement, shown in Figure 2, imply that they might have different dowel resistance characteristics. Since the model had

fewer cracks and a relatively larger crack width than the prototype, this led to more pronounced kinking and less buckling resistance of the model reinforcement. As the failure of the model wall occurred through the buckling and subsequent rupturing of its edge member reinforcement, the importance of maintaining similitude of dowel action and particularly inelastic buckling characteristics of reinforcing steel is obvious for a correct representation of structural failure by the model.

7. CONCLUSIONS AND RECOMMENDATIONS

7.1 GENERAL CONCLUSIONS

To achieve a "true" model careful attention is required in selecting model materials which simulate the responses of the structural materials very closely. The stress-strain constitutive relationships of the constituent materials as affected by the *stress state, level* and *history,* as well as their failure characteristics and physical properties (i.e. volumetric change characteristics), should be identical in model and prototype.

This is very difficult, if at all possible, to achieve in the case of reinforced concrete. Although many problems were confronted in the simulation of the so-called linear elastic behavior, the problems and difficulties increased substantially (1) as model scale was reduced and (2) as the simulation of inelastic limit state responses of the structure was desired, particularly when damageability and local, partial, and complete collapse limit state inelastic responses involving different failure modes of the structure constituted the main phenomena being modelled.

7.1.1 Modelling Linear Elastic Response

In modelling the so-called linear elastic response of the reinforced concrete structure, simulation of the geometry (except for the pattern of surface deformation, i.e., bond) and linear elastic characteristics of reinforcement (E_s and ν_s) was relatively simple. It was also possible to achieve for the model concrete similar low stress level response characteristics, such as E_c and ν_c.* The tensile strength and bond characteristics of the prototype concrete, however, could not be simulated by micro-concrete, which also had substantially larger shrinkage. All of these concrete characteristics affected cracking and, consequently, resulted in some disagreement between prototype and model responses when these responses involved cracking.

*It is important to note that even if E_c and ν_c of the full-scale concrete are perfectly simulated by the micro-concrete it does not follow that the shear modulus of rigidity, G, will also be simulated, since the relation existing between E, G, and ν for Hookean homogeneous and isotropic material is not valid for concrete [3]. The proper simulation of the shear modulus of rigidity should be considered in addition to E_c and ν_c for the study of so-called linear response of R/C models.

Even if it were possible to attain perfect agreement between the tensile strength, bond, and volumetric change characteristics of the prototype concrete and the model concrete, this would not necessarily result in identical cracking patterns and proportional crack widths in the prototype and model structures, since (1) the strain rate and (2) the strain gradient, two important parameters affecting the response of concrete, are inherently larger in a scaled model. Strain rate in dynamic testing is larger by the factor $\sqrt{L_r}$, while strain gradient is larger by the factor L_r in a "true" replica model. Both of these parameters can affect the distribution and width of cracking significantly.

7.1.2 Modelling Inelastic Response

When a correct simulation of the inelastic behavior of the structure is required, the difficulties increase significantly. It then becomes necessary to attain similitude in the complete stress-strain relation of reinforcing steel under any possible strain history. Also, the concrete constitutive relations as well as the bond characteristics for the model material should agree with those of the prototype materials up to the largest expected level of strain.

The smaller the scale the more difficult is the attainment of material response similitude.

In the case of steel, the mechanical characteristics which were required to be similar besides those discussed for the elastic range were (1) yielding stress, f_y; (2) plastic plateau, $(\epsilon_{STH} - \epsilon_y)$; (3) initial strain hardening modulus, E_{STH}; (4) maximum stress, f_u; (5) maximum strain, ϵ_u; (6) hysteretic response characteristics (kinematic hardening and Bauschinger effect); and (7) kinking characteristics.

In the case of concrete, in addition to E_c, ν, and f_t, the characteristics for which similitude between model and prototype material was observed to be necessary were: (1) maximum stress, f_c', (2) strain at maximum stress, ϵ_o, (3) average slope of the descending branch of the stress-strain relation, (4) ultimate (spalling) strain, (5) bond characteristics, and (6) the effects of stress state (i.e., effect of confinement, stress rate, stress gradient, and stress history on (1) to (5)).

The state-of-the-art in the design and fabrication of model materials, particularly micro-concrete, was assessed to be inadequate to achieve the desired similitude in many of the listed aspects of material response. It is, therefore, important to predict accurately the regions of the structure where inelastic behavior would be expected as well as those critical components and regions which would control the behavior of the structure. In such regions, particular care in the reproduction of the critical material response characteristics should be pursued.

7.1.3 Importance of Integrated Analytical and Experimental Studies

The problems confronted in these studies conducted to achieve true similitude in the mechanical characteristics and properties of the structural materials reaffirm the importance of conducting integrated analytical and experimental studies. Although it was not possible to predict the real response of the structure exactly, results from analyses using available computer programs gave a good idea of the mechanism controlling the inelastic behavior and permitted the detection of critical regions. Efforts to obtain as true simulation as possible of the characteristics of the material in these regions resulted in economically achieving an acceptable simulation.

7.2 SPECIFIC CONCLUSIONS

The outcome of the efforts to conduct experimental analyses of the serviceability, damageability, and collapse limit state responses of the structure was adversely affected by the different loading schemes, loading programs and boundary conditions of the prototype and model structures. The influence of the following material response characteristics was observed to be significant in attaining a correct simulation of the different limit state response characteristics of the structure.

7.2.1 Response Characteristics of Reinforcing Steel

(1) Errors in simulating the deformation pattern of the surface and cross-sectional area of prototype reinforcement could not be totally eliminated. These affected the similitude in the amount of steel at the cross section and in the yield strength of the sections.

Similitude in the yield strengths of the model and prototype cross sections was better achieved by using the force-strain rather than the stress-strain relations of the reinforcing bars, as these were duplicated on a one-to-one basis, and a precise evaluation of the effective cross-sectional areas of the model reinforcement was not possible.

(2) A good correlation in the modulus of elasticity, yield strength, and maximum strength of the reinforcing bars was achieved.

(3) The bond characteristics of the model column reinforcement were evaluated to be better than those of the prototype.

(4) Considerable discrepancies in the yield plateau and initial strain hardening characteristics of the prototype and model reinforcements could not be eliminated. The stress-strain responses of the reinforcement in the edge members of the main shear wall, however, were assessed to be the critical material responses for similitude in structural response. The agreement in yield strength as well as the yield plateau and strain hardening characteristics of the reinforcement in the wall edge members was considerably closer because of special efforts undertaken to satisfy the similitude requirements at these most critical regions of the structure.

(5) The hysteresis characteristics of reinforcement could not be incorporated in the efforts to satisfy similitude.

7.2.2 Response Characteristics of Concrete

Only the monotonic stress-strain relations of unconfined concrete could be studied. Hysteretic responses or responses affected by confinement could not be included in the efforts to achieve similitude.

(1) The correlation in the compressive strength was not as desired because of the significant increase in the strength of the micro-concrete with age. This was not expected and there was practically no corresponding increase in strength of the prototype concrete after 28 days.

(2) The tensile strength of micro-concrete was of the order of twice the corresponding strength of the prototype concrete. Although this is a recognized inherent characteristic of micro-concrete, it could not be avoided without drastic changes in the mix.

(3) A secant modulus of elasticity of concrete, measured at 45 percent of the maximum strength, agreed well between the model and the prototype materials.

(4) The strain at maximum strength of the micro-concrete was considerably higher than the corresponding strain in the prototype concrete. Larger deformability is an inherent characteristic of micro-concrete.

(5) The shrinkage of micro-concrete was assessed to be many times higher than the shrinkage of the prototype concrete, leading to distorted initial internal stresses which affected the initial response of the model.

(6) The variations in concrete strength decreased with the aging of the concrete.

(7) The splitting tensile strength of concrete (ASTM C-496), as obtained from 3-in. by 6-in. cylinders, was the same as obtained from flexural strengths tests of 5-in. by 6-in. beams, 20-in. long and tested in third point loading, with a constant moment region along a 6-in. length of the beam (ASTM C-683). Although these beams are expected to yield generally higher tensile strength than splitting strengths of 6-in. by 12-in. cylinders, the smaller 3-in. by 6-in. cylinders developed splitting strengths equalling the values obtained from the beams. Due to the relatively larger cross-sectional dimensions of the beams when compared with the 3-in. by 6-in. cylinders, the differential shrinkage along a typical cross section of the beam should be more than that of the cylinder. This should be expected to lead to larger initial tensile stresses in beam cross sections, as compared to the smaller cylinder cross sections, explaining why tensile strength from beams were not higher than those obtained from cylinders.

(8) The correct cylinder size, which would yield stress-strain characteristics representative of the characteristics of the material in the critical elements and regions of the scaled model structure, is a problem requiring further research. As an example, if the concrete of the

1.57-in. (4 cm) thick wall panel is considered to be the critical material in the model, and therefore reliable stress-strain characteristics are required, what would be the correct size of a cylinder used to sample the micro-concrete? Since smaller samples characteristically yield higher strength, the size of the sample cylinder tested must be taken into account when determining the strength of the concrete in the model from the strength of the cylinder. The effects of size in testing of concrete of both compressive and tensile strength determination require further research.

8. REFERENCES

1. AIJ Standard for Structural Calculation of R/C Structures, Architectural Institute of Japan, Revised 1979, 3-2-19, Ginza, Chuo-ku, Tokyo, Japan.

2. Aktan, A. E. and Bertero, V. V., "1/5 Scale Model of the 7-Story R/C Frame-Wall Test Building: Design and Construction," Proceedings of the Third Joint Technical Coordinating Committee, U.S.-Japan Joint Cooperative Earthquake Research Program, Tsukuba, Japan, July 1982.

3. Aktan, A. E., Bertero, V. V., Chowdhury, A. A., and Nagashima, T., "Experimental and Analytical Predictions of the Mechanical Characteristics of a 7-Story 1/5 Scale Model R/C Frame-Wall Building Structure," Earthquake Engineering Research Center, *Report No. UCB/EERC-83/13,* University of California, Berkeley, 1983.

4. Bertero, V. V., Aktan, A. E., and Clyde, D., "1/5 Scale Model of the 7-Story R/C Test Building: Model Materials," Proceedings of the Third Joint Technical Coordinating Committee, U.S.-Japan Joint Cooperative Earthquake Research Program, Tsukuba, Japan, July 1982.

5. Charney, A. F. and Bertero, V. V., "An Evaluation of the Design and Analytical Seismic Response of a Seven-Story Reinforced Concrete Frame-Wall Structure," Earthquake Engineering Research Center, *Report No. UBC/EERC-82/08,* University of California, Berkeley, August 1982.

6. Harris, H. G., Sabnis, G. M., and White, R. N., "Small Scale Direct Models of Reinforced and Prestressed Concrete Structures," *Report No. 326,* Department of Structural Engineering, School of Civil Engineering, Cornell University, Ithaca, New York, September 1966.

7. Harris, H. G., Bertero, V. V., and Clough, R. W., "One-Fifth Scale Model of a Seven-Story Reinforced Concrete Frame-Wall Building Under Earthquake Loading," Paper presented at and published in the Proceedings of the Seminar on Dynamic Modelling of Structures, Joint I. Struct. E./B.R.E., Building Research Station, Garston, England, November 1981.

8. Harris, H. G., Editor, "Dynamic Modelling of Concrete Structures," *Publication SP-73,* American Concrete Institute, Detroit, 1982.

9. Monkarz, P. D. and Krawinkler, H., "Theory and Application of Experimental Model Analysis in Earthquake Engineering," *Report No. 50,* The John A. Blume Earthquake Engineering Center, Department of Civil Engineering, Stanford University, Stanford, California, June 1981.

10. Noor, F. A. and Wijayasri, S., "Modelling the Stress-Strain Relationship of Structural Concrete," *Magazine of Concrete Research,* Vol. 34, No. 116, March 1983.

11. U.S.-Japan Planning Group, Cooperative Research Program Utilizing Large-Scale Testing Facilities, "Recommendations for a U.S.-Japan Cooperative Research Program Utilizing Large-Scale Testing Facilities," *Report No. UCB/EERC-79/26,* Earthquake Engineering Research Center, University of California, Berkeley, September 1979.

12. Wight, J. K. and Nakata, S., "Construction of the Full-Scale Seven-Story Reinforced Concrete Test Structure," Proceedings of the Second Joint Technical Coordinating Committee, U.S.-Japan Joint Cooperative Earthquake Research Program, Tsukuba, Japan, July 1982.

TABLES

TABLE 1. STRESS-STRAIN CHARACTERISTICS OF PROTOTYPE STEEL*

Bar Size	Test Series	E ksi	f_y ksi	ϵ_{STH} in/in	E_{STH} ksi	f_u ksi	ϵ_u in/in
D22	1	26300	57.79	-	-	88.91	0.242
	2		50.21	0.0125	915.97	81.78	0.191
D19	1	29500	52.23	-	-	62.24	0.229
	2		51.91	0.0165	785.12	81.50	0.214
D10	1	26200	52.55	-	-	77.33	0.204
	2		55.04	0.0185	735.33	81.21	0.210

*All quantities are average of three tests except E, which is the average of six tests.

E = modulus of elasticity

f_y = yield stress

ϵ_{STH} = strain at onset of strain hardening

E_{STH} = strain hardening modulus

f_u = maximum tensile stress

ϵ_u = ultimate strain

1 ksi = 6.89 MPa

1 in. = 25.4 mm

TABLE 2. AREA* OF PROTOTYPE AND MODEL REINFORCEMENT

Bars	Prototype Area	Area Required for Similitude	Obtained Model Area	% Error
Column/ Edge Member	(D22 Bar) 0.5890	0.0236	(PCA/D2.5 Bar) 0.0214	(-) 9.17
Beam	(D19 Bar) 0.4394	0.0176	(PCA/D2 Bar) 0.0186	(+) 5.80
Wall/Slab/ Ties/Stirrups	(D10 bar) 0.1217	0.00487	(Knurled Wire 14 Gauge) 0.00464	(-) 4.68

*All areas are given in square inches.

1 in. = 25.4 mm

TABLE 3. CROSS-SECTIONAL AREAS* OF MODEL REINFORCEMENT OBTAINED BY DIFFERENT TECHNIQUES

Bar	Area Based on Volume/Length	Area Based on Direct Measurement		Effective Area
		Maximum	Minimum	
PCA D2.5	0.0255	0.0238	0.0203	0.0214
PCA D2.0	0.0193	0.0190	0.0181	0.0186
14 Gauge Wire, Knurled	0.0051	0.0047	0.0041	0.0046

*All areas are given in square inches.

1 in ^{2} = 6.45 cm ^{2}

TABLE 4. STRESS-STRAIN CHARACTERISTICS OF MODEL STEEL

Bar	Statistics	E ksi	f_y ksi	ϵ_{STH} in/in	E_{STH} ksi	f_u ksi	ϵ_u in/in
PCA D2.5 Columns	Upper Bound*		60.58	0.0172	388.20	81.74	0.2386
	Lower Bound*		58.16	0.0128	357.60	76.26	0.1856
	Mean	28700	59.37	0.0150	372.90	79.00	0.2121
	Standard Deviation	3900	4.23	0.0068	53.33	9.58	0.0456
PCA D2 Beams	Upper Bound*		54.80	0.0260	506.00	72.40	0.216
	Lower Bound*		54.20	0.0250	482.00	72.00	0.202
	Mean	28900	54.50	0.0255	494.00	72.20	0.209
	Standard Deviation	4000	1.06	0.0018	48.60	0.80	0.019
14 Gauge Wire Walls/ Slabs	Upper Bound*		62.72	0.0337	236.00	79.51	0.1918
	Lower Bound*		60.42	0.0283	222.20	78.84	0.1758
	Mean	28800	61.57	0.0310	229.10	79.18	0.1838
	Standard Deviation	3200	3.21	0.0073	19.11	0.94	0.0207

*90% confidence limit

E = modulus of elasticity

f_y = yield stress

ϵ_{STH} = strain at onset of strain hardening

E_{STH} = strain hardening modulus

f_u = maximum tensile stress

ϵ_u = ultimate strain 1 ksi = 70.22 kg/cm ^{2} = 6.89 MPa

TABLE 5. CONCRETE MIXES USED IN THE PROTOTYPE					
Story	Design Strengths (ksi)	Materials (lbs/cu. yd.)			
		Cement	Water	Sand	Gravel*
1 to 4	3.63	551.17	281.48	1336.62	1682.16
5 to 7	3.84	559.59	266.31	1309.65	1752.95

*Maximum size = 1-inch round aggregate.
1 ksi = 70.22 kg/cm ^{2} = 6.89 MPa
1 lb/cu. yd. = 0.592 kg/m ^{3}
1 inch = 25.4 mm

TABLE 6. SLUMP TESTS		
Location	Slump (in.)	
	Model	Prototype
First Floor	7.5	7.6
Second Floor	7.5	7.5
Third Floor	8.5	7.4
Fourth Floor	8.5	7.4
Fifth Floor	8.8	7.4
Sixth Floor	8.3	7.4
Seventh Floor	8.0	7.6
Footing	5.5	6.5
Column Stubs	5.5	0.0

Average slump (model) = 8.1 in.
Average slump (prototype) = 7.5 in.
Average slump excludes slump of footing and/or column stubs.
1 inch = 25.4 mm

TABLE 7. MECHANICAL CHARACTERISTICS OF PROTOTYPE CONCRETE

Location	Age (days)	f_{cmax} (ksi)	ϵ_0 (in/in)	$E_{1/3 f_{cmax}}$ (ksi)	$E_{0.45 f_{cmax}}$ (ksi)	f_{sp} (ksi)
First Floor	28 145	3.60 4.11	0.00218	3390	3150	0.34
Second Floor	28 132	3.68 4.15	0.00240	3360	3110	0.35
Third Floor	28 119	3.37 3.90	0.00228	3140	2950	0.34
Fourth Floor	28 111	3.43 4.13	0.00225	3000	2930	0.33
Fifth Floor	28 98	3.56 4.20	0.00210	3330	3150	0.34
Sixth Floor	28 87	2.05	0.00185	1980		0.19
Seventh Floor	28 67	2.69	0.00192	2470		0.19

*f_{sp} = tensile stress from split cylinder test

1 ksi = 70.22 kg/cm ^{2} = 6.89 MPa

1 inch = 25.4 mm

TABLE 8. CONCRETE MIX USED IN 1/5 SCALE MODEL

Materials	Parts by Weight	Weight per Cubic Yard, lbs.
Water	0.67	400
Cement, Lone Star Type I-II	1.00	597
Coarse Sand*, Radum Top	3.75	1139
Coarse Gravel*, Radum (1/4 in.)	1.00	597
Admixture, Pozzolith-300R	4 oz./100 lbs.	-

*Saturated surface-dry condition.

1 lb. = 0.453 kg = 4.45N

1 lb/cu. yd. = 0.592 kg/m ^{3}

TABLE 9. MECHANICAL CHARACTERISTICS OF MODEL CONCRETE*

Location	Age, days	Sample Size	$\bar{f}_{cmax}$ ksi	$\sigma_{f_{cmax}}$ ksi	$\bar{\epsilon}_0$ in/in	σ_{ϵ_0} in/in	$\bar{E}_{0.45f_{cmax}}$ ksi	$\sigma_{E_{0.45f_{cmax}}}$ ksi
Footing	254	1	5.44	0.0	0.00340	0.0	2970	0.0
Column Stubs	254	1	6.51	0.0	0.00330	0.0	3490	0.0
First Floor	28	3	3.61	0.116	0.00250	0.000325	2800	123.94
	216	2	5.68	0.032	0.00350	0.000141	3160	183.85
	456	4	5.67	0.215	0.00380	0.000206	2940	61.22
Second Floor	28	3	4.18	0.141	0.00292	0.000157	2940	109.70
	208	2	5.66	0.0	0.00350	0.000283	3380	158.39
	446	3	5.70	0.026	0.00355	0.000132	2990	123.52
Third Floor	28	3	3.93	0.146	0.00282	0.000274	3340	63.17
	195	2	5.99	0.0	0.00350	0.0	3380	28.99
	434	4	5.59	0.465	0.00345	0.000208	3070	125.55
Fourth Floor	28	3	3.68	0.142	0.00261	0.000153	2930	85.91
	187	2	5.26	0.0	0.00320	0.0	3320	229.10
	425	4	5.54	0.156	0.00361	0.000189	2930	81.18
Fifth Floor	28	3	4.75	0.086	0.00283	0.000293	3080	61.65
	175	1	5.88	0.0	0.00320	0.0	3530	0.0
	413	2	5.50	0.110	0.00330	0.000141	3030	22.63
Sixth Floor	28	2	4.16	0.040	0.00288	0.000354	2880	11.31
	168	1	5.48	0.0	0.00350	0.0	3290	0.0
	408	3	5.45	0.263	0.00344	0.000351	2970	59.77
Seventh Floor	28	3	4.87	0.122	0.00284	0.000290	3060	93.40
	159	1	5.84	0.0	0.00290	0.0	3020	0.0
	399	4	5.80	0.421	0.00353	0.000340	3150	154.00

*As determined from load control tests of 3-in. x 6-in. field cured cylinders.

$\bar{f}_{cmax}$, $\sigma_{f_{cmax}}$ = mean and standard deviation of maximum concrete stress

$\bar{\epsilon}_o$, σ_{ϵ_o} = mean and standard deviation of strain at maximum concrete stress

$\bar{E}_{0.45f_{cmax}}$, $\sigma_{E_{0.45f_{cmax}}}$ = mean and standard deviation of the secant modulus at 45% of maximum concrete stress

1 inch = 25.4 mm

1 ksi = 70.22 kg/cm ^{2} = 6.89 MPa

TABLE 10. THE MEAN MECHANICAL CHARACTERISTICS OF THE MODEL CONCRETE FOR ALL SEVEN FLOORS

Age, days	$\bar{f}_{cmax}$ ksi	$\sigma_{f_{cmax}}$ ksi	$\bar{\epsilon}_0$ in/in	σ_{ϵ_0} in/in	$\bar{E}_{0.45f_{cmax}}$ ksi	$\sigma_{E_{0.45f_{cmax}}}$ ksi
28	4.168	0.456	0.00277	0.000169	3004	170.00
159-216	5.684	0.249	0.00333	0.000236	3292	162.40
399-456	5.606	0.123	0.00350	0.000170	3010	80.68

$\bar{f}_{cmax}$, $\sigma_{f_{cmax}}$ = mean and standard deviations of maximum concrete stress

$\bar{\epsilon}_o$, σ_{ϵ_o} = mean and standard deviations of strain at maximum concrete stress

$\bar{E}_{0.45f_{cmax}}$, $\sigma_{E_{0.45f_{cmax}}}$ = mean and standard deviations of secant modulus at 45% of maximum concrete stress

1 inch = 25.4 mm

1 ksi = 70.22 kg/cm ^{2} = 6.89 MPa

TABLE 11. TENSILE STRENGTH OF MODEL CONCRETE

Location	Split Cylinder* f_t (psi)	Beam Tests f_t (psi)	
		(1)	(2)
First Story	729 (9.67)**	760 (10.04)	760 (10.03)
Second Story	748 (9.94)	850 (11.31)	860 (11.41)
Third Story	785 (10.15)	715 (9.26)	720 (9.33)
Fourth Story	739 (10.19)	660 (9.07)	680 (9.32)
Fifth Story	784 (10.22)	755 (9.82)	790 (10.27)
Sixth Story	694 (9.37)	800 (10.83)	705 (9.56)
Seventh Story	750 (9.79)	790 (10.34)	630 (8.22)
Column Stub	684 (8.48)		
Footing	694 (9.41)		

*Average of three tests.

**Values in brackets indicate factor of $\sqrt{f'_c}$ where f'_c was the average maximum cylinder strength of concrete obtained for the corresponding story of the structure at time of tensile strength test, and as given in Table 9.

1 psi = 0.0702 kg/cm ^{2} = 6.89 kPa = 0.0069 MPa

TABLE 12. FORCE AND STRAIN RESPONSE CHARACTERISTICS FOR PROTOTYPE AND MODEL REINFORCEMENT

Reinforcement	E_p (ksi)	E_m (ksi)	F_{yp}** (kips)	F_{ym} (kips)	ε_{STHP} (in/in)	ε_{STHM} (in/in)	E_{STHP} (ksi)	E_{STHM} (ksi)	F_{up}** (kips)	F_{um} (kips)	ε_{up} (in/in)	ε_{um} (in/in)
Columns	26300	28700	1.183	1.271	0.0125	0.0150	916	373	1.927	1.691	0.191	0.2121
Beams	29500	28900	0.912	1.014	0.0165	0.0255	785	495	1.432	1.343	0.214	0.2090
Walls/ Slabs	26200	28800	0.258	0.286	0.0185	0.0310	735	229	0.385	0.367	0.210	0.1838

** F_{yp} and F_{up} were divided by $(L_p/L_m)^2$.

NOTES: Prototype properties were from series 2 tests. Mean values were used for model reinforcement properties.

E_p, E_m = Modulus of elasticity for prototype and model.

E_{STHP}, E_{STHM} = Strain hardening modulus for prototype and model.

F_{yp}, F_{ym} = Yield force of prototype and model.

F_{up}, F_{um} = Maximum tensile force for prototype and model.

$\varepsilon_{STHP}, \varepsilon_{STHM}$ = Strain at onset of strain hardening.

$\varepsilon_{up}, \varepsilon_{um}$ = Ultimate strain for prototype and model.

1 inch = 25.4 mm
1 ksi = 70.82 kg/cm^2 = 6.89 MPa
1 kip = 453 kg = 4450 N

TABLE 13. COMPARISON OF MAIN RESPONSE PARAMETERS OF PROTOTYPE AND MODEL REINFORCEMENT

Reinforcement	$\frac{E_m}{E_p}$	$\frac{F_{ym}}{F_{yp}}$	$\frac{\epsilon_{STHM}}{\epsilon_{STHP}}$	$\frac{E_{STHP}}{E_{STHM}}$	$\frac{F_{um}}{F_{up}}$	$\frac{\epsilon_{um}}{\epsilon_{up}}$
Columns	1.091	1.074	1.20	0.407	0.878	1.110
Beams	0.980	1.112	1.545	0.629	0.938	0.977
Walls/ Slabs	1.099	1.067	1.676	0.311	0.953	0.875

E_p, E_m = modulus of elasticity for prototype and model

F_{yp}, F_{ym} = yield force of prototype and model

ϵ_{STHP}, ϵ_{STHM} = strain at onset of strain hardening of prototype and model

E_{STHP}, E_{STHM} = strain hardening modulus for prototype and model

F_{um}, F_{up} = maximum tensile force for prototype and model

ϵ_{um}, ϵ_{up} = ultimate strain for prototype and model

FIGURES

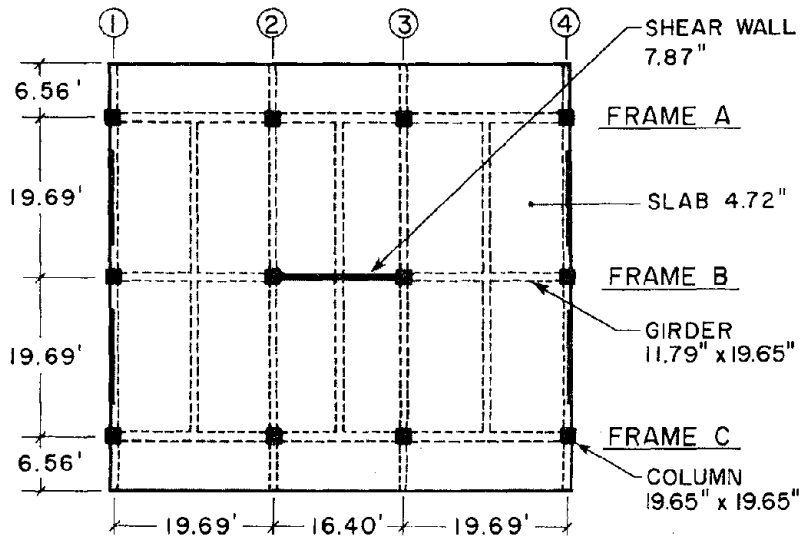

(a) PLAN OF PROTOTYPE STRUCTURE

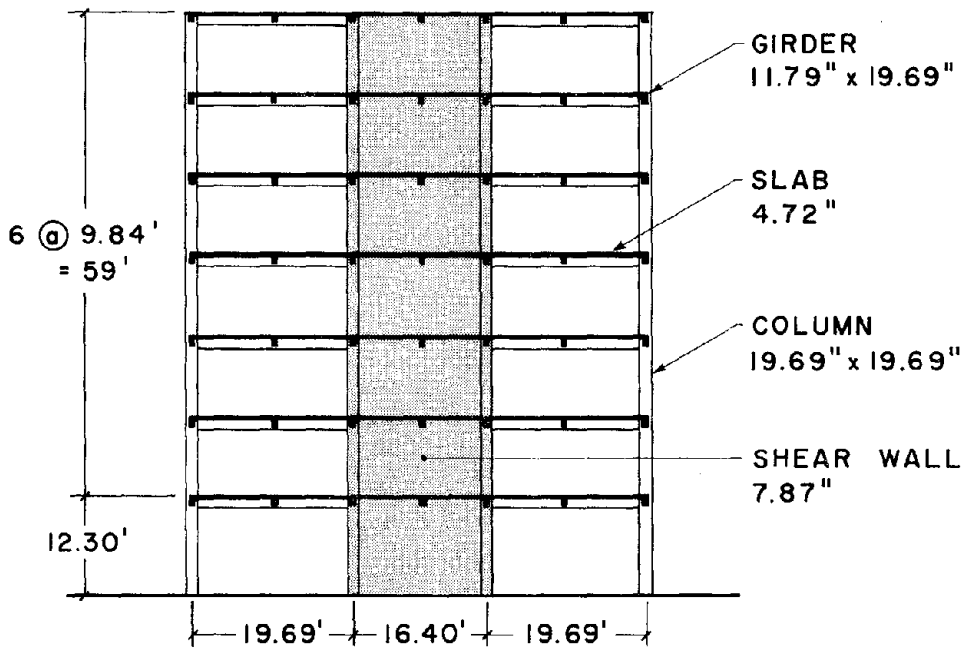

(b) SECTION OF PROTOTYPE FRAME B

FIG. 1 PLAN AND ELEVATION OF TEST BUILDING.
1 in. = 25.4 mm 1 ft = 0.305 m

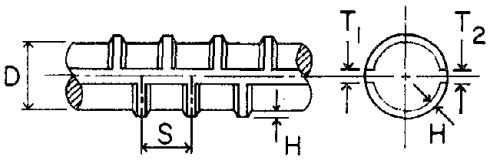

BAR	DIAMETER		S	H	$T_1 + T_2$
	in.	mm	mm	mm	mm
D10	0.38	9.53	6.7	0.4-0.8	7.5
D19	0.75	1.91	13.4	1.0-2.0	15.0
D22	0.87	22.2	15.5	1.1-2.2	17.5

(a) PROTOTYPE REINFORCING BARS

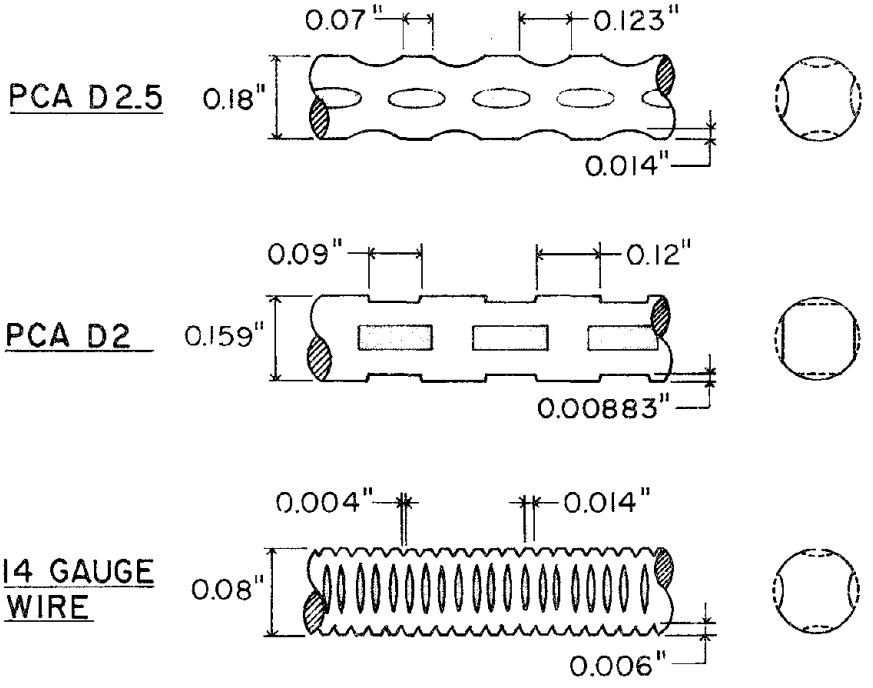

(b) MODEL REINFORCEMENT

FIG. 2 GEOMETRIC CHARACTERISTICS OF THE REINFORCING BARS USED IN THE PROTOTYPE AND MODEL. 1 in. = 25.4 mm

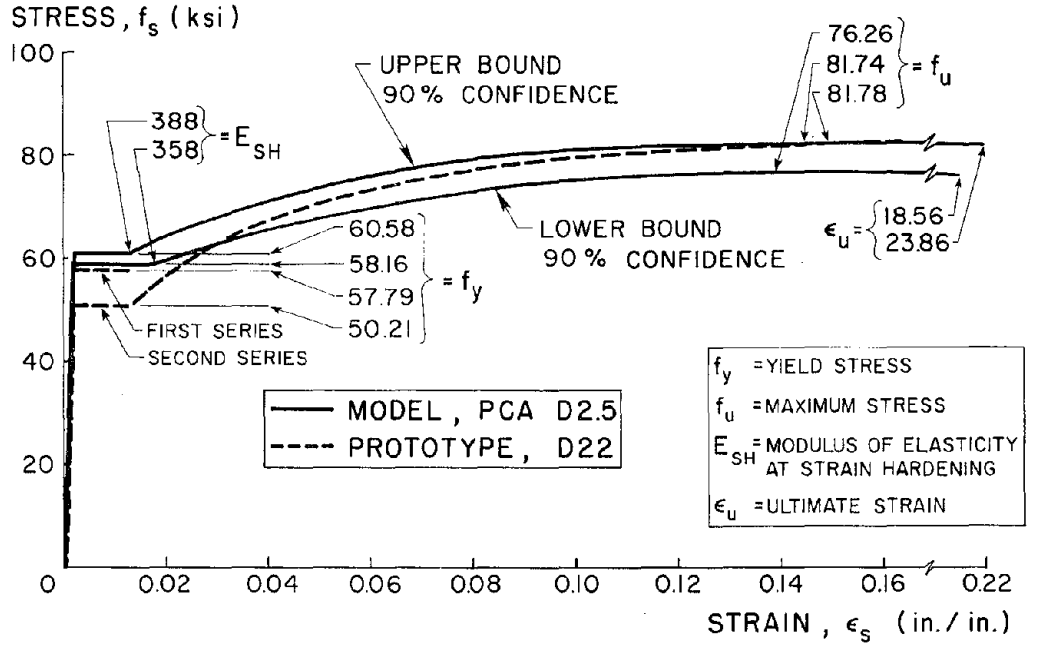

FIG. 3 STRESS-STRAIN RELATIONS FOR COLUMN REINFORCEMENT.
1ksi = 6.9 MN/m^2 1 in. = 25.4 mm

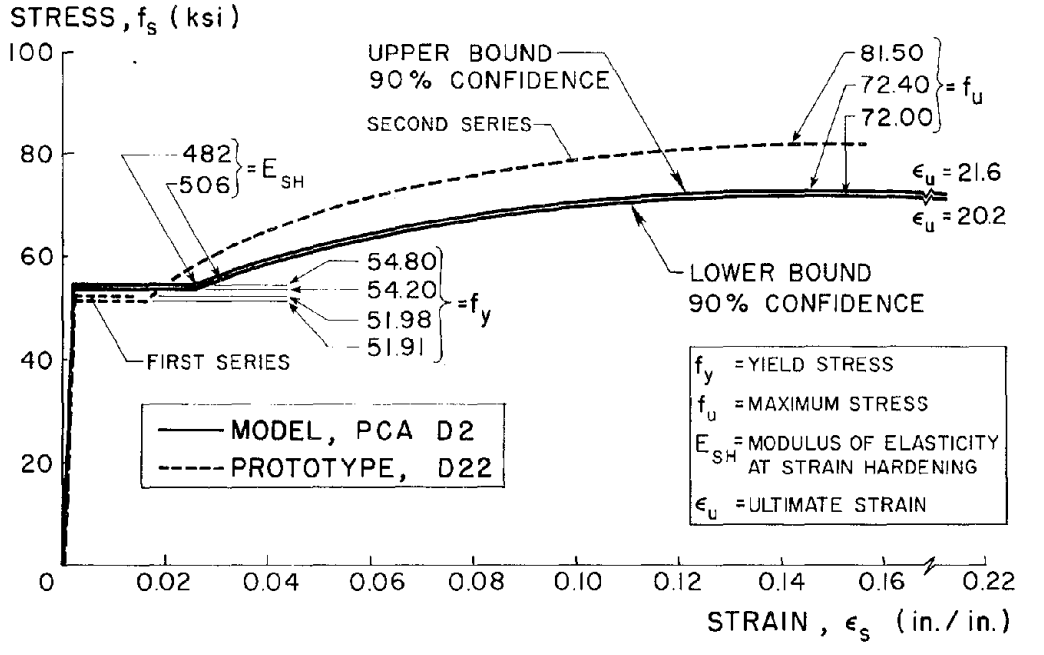

FIG. 4 STRESS-STRAIN RELATIONS FOR BEAM REINFORCEMENT.
1 ksi = 6.9 MN/m^2 1 in. = 25.4 mm

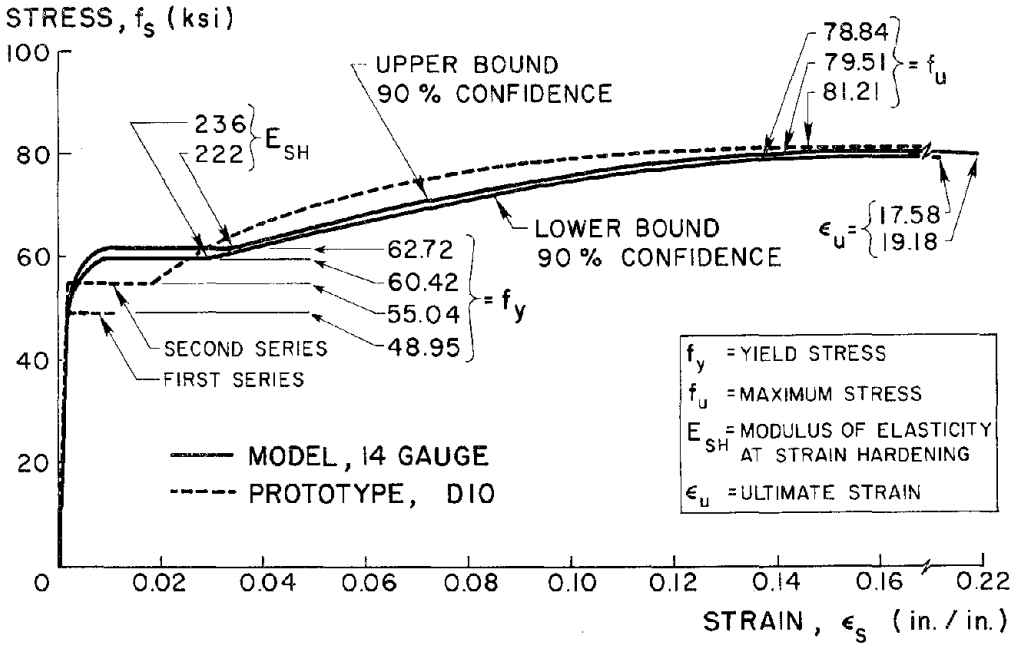

FIG. 5 STRESS-STRAIN RELATIONS FOR WALL, SLAB, TIE AND STIRRUP REINFORCEMENT. 1ksi = 6.9 MN/m^2 1 in. = 25.4 mm

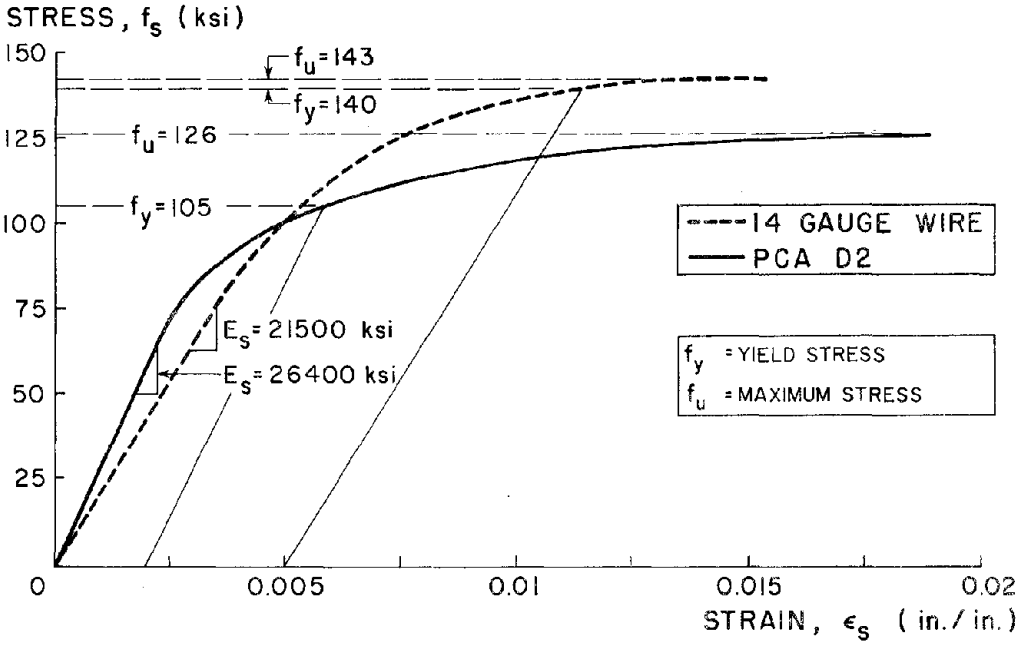

FIG. 6 STRESS-STRAIN RELATIONS FOR THE ORIGINAL (VIRGIN) 14 GAUGE WIRE AND PCA/D2 REINFORCING BARS.
1 ksi = 6.9 MN/m^2 1 in. = 25.4 mm

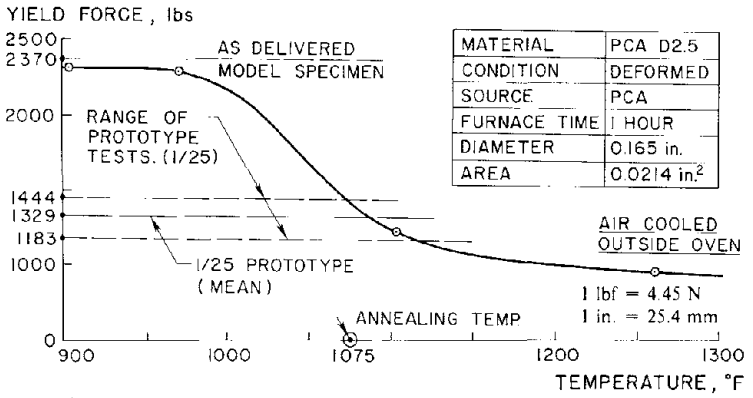

FIG. 7 YIELD FORCE VS. 1 HOUR OVEN TEMPERATURE RELATION FOR COLUMN REINFORCEMENT.

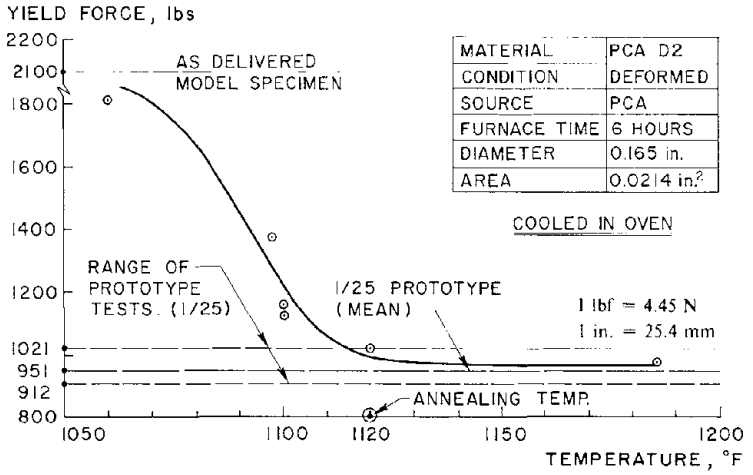

FIG. 8 YIELD FORCE VS. 6 HOUR OVEN TEMPERATURE RELATION FOR BEAM REINFORCEMENT.

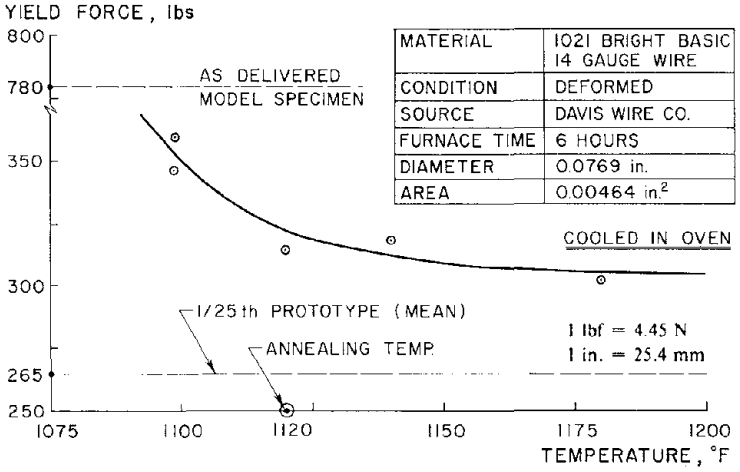

FIG. 9 YIELD FORCE VS. 6 HOUR OVEN TEMPERATURE RELATION FOR WALL AND SLAB REINFORCEMENT.

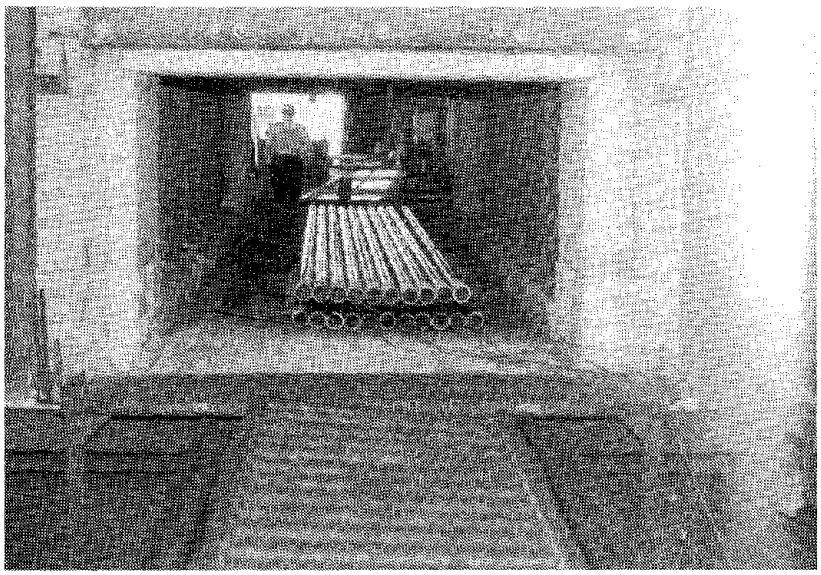

(a) VIEW OF 3 INCH STEEL TUBES FILLED WITH THE REINFORCING BARS IN THE OVEN.
1 in. = 25.4 mm

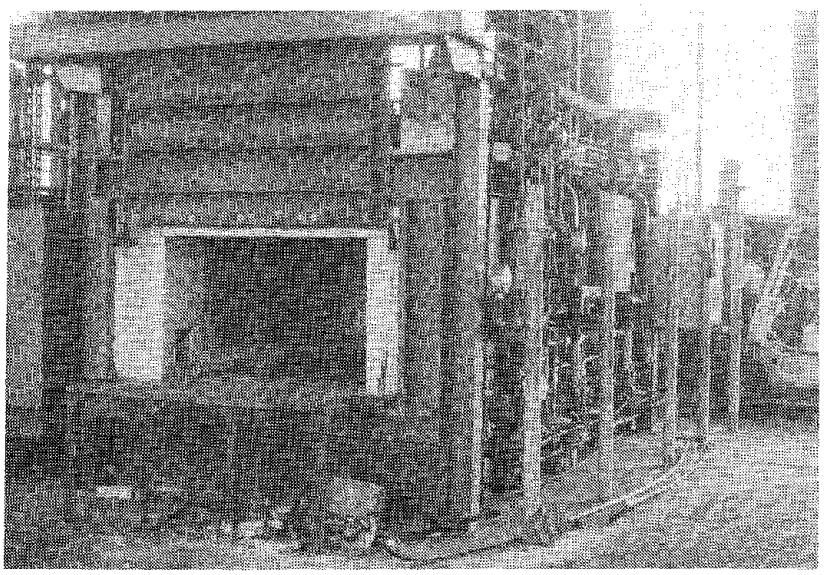

(b) SIDE VIEW OF OVEN

FIG. 10 VIEWS OF LINDBERG HEAT TREATMENT CO. (OAKLAND) OVEN WHERE HEAT TREATMENT OF MODEL REINFORCEMENT WAS CARRIED OUT.

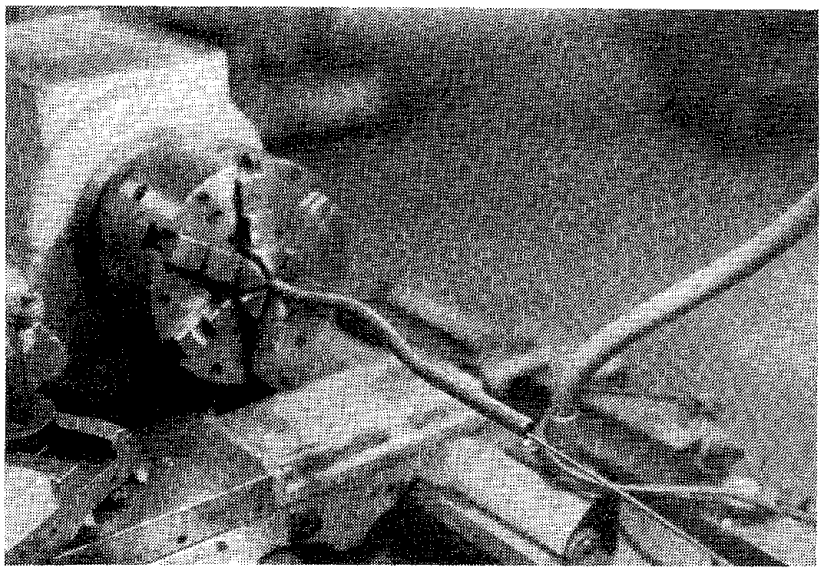

FIG. 11 PHOTOGRAPH ILLUSTRATING STRAIGHTENING PROCESS FOR ANNEALED WIRE USING A LATIIE AND A BENT TUBE.

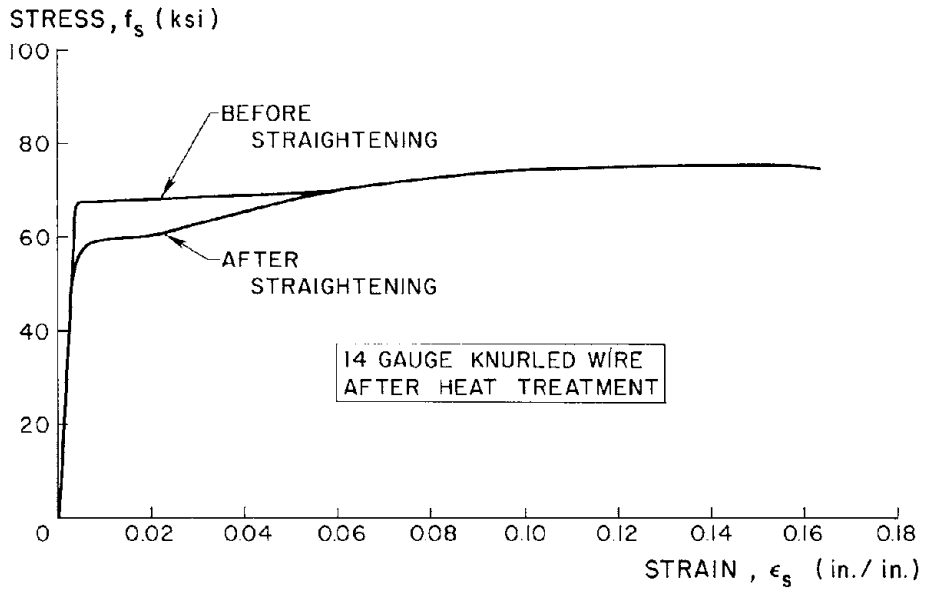

FIG. 12 EFFECT OF STRAIGHTENING WALL AND SLAB REINFORCEMENT AFTER HEAT TREATMENT. 1ksi = 6.9 MN/m^2 1 in. = 25.4 mm

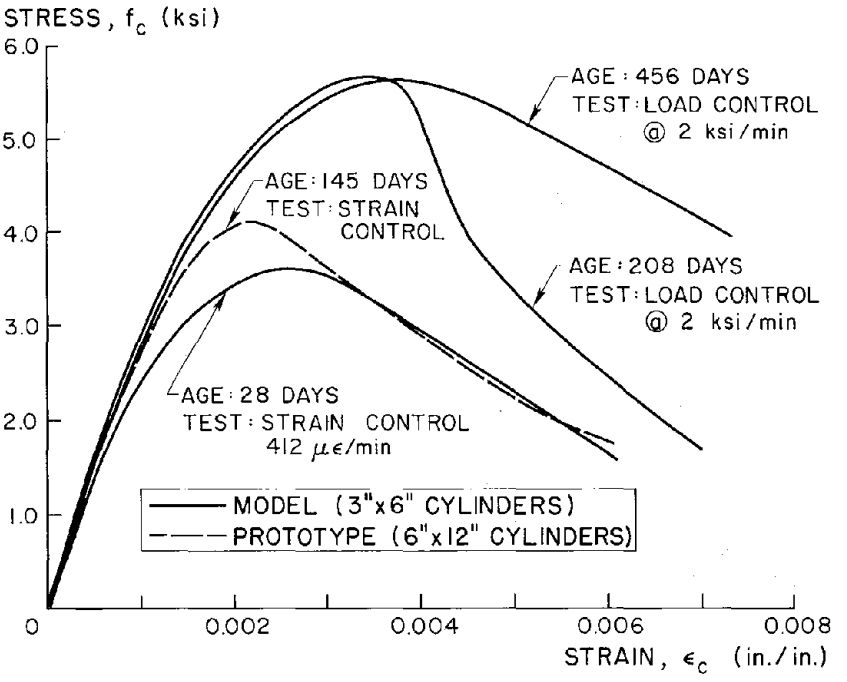

FIG. 13 STRESS-STRAIN RELATIONSHIP OF CONCRETE IN FIRST STORY.
1 ksi = 6.9 MN/m^2 1 in. = 25.4 mm

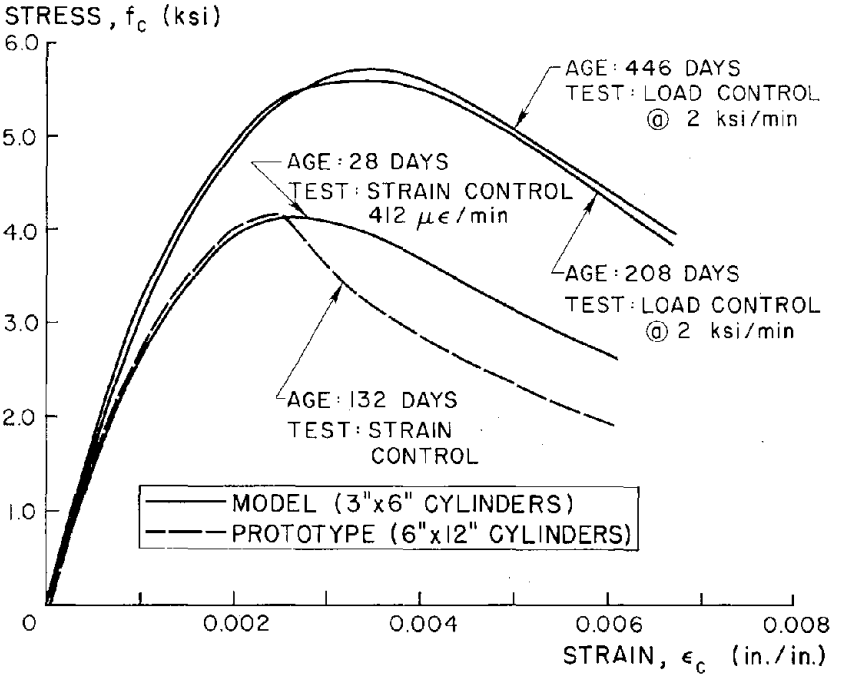

FIG. 14 STRESS-STRAIN RELATIONSHIP OF CONCRETE IN SECOND STORY.
1 ksi = 6.9 MN/m^2 1 ft = 0.305 m

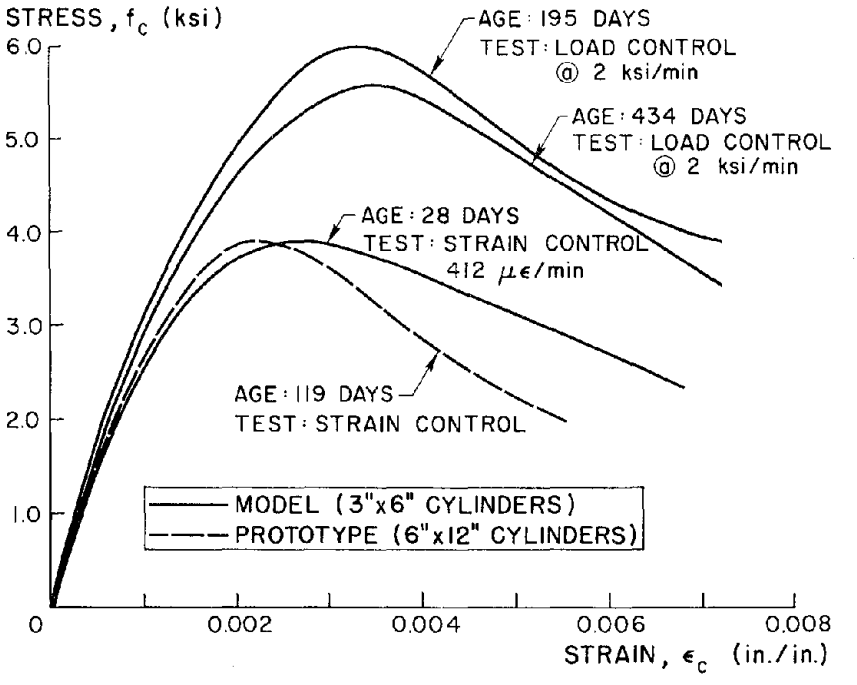

FIG. 15 STRESS-STRAIN RELATIONSHIP OF CONCRETE IN THIRD STORY.
1 ksi = 6.9 MN/m^2 1 in. = 25.4 mm

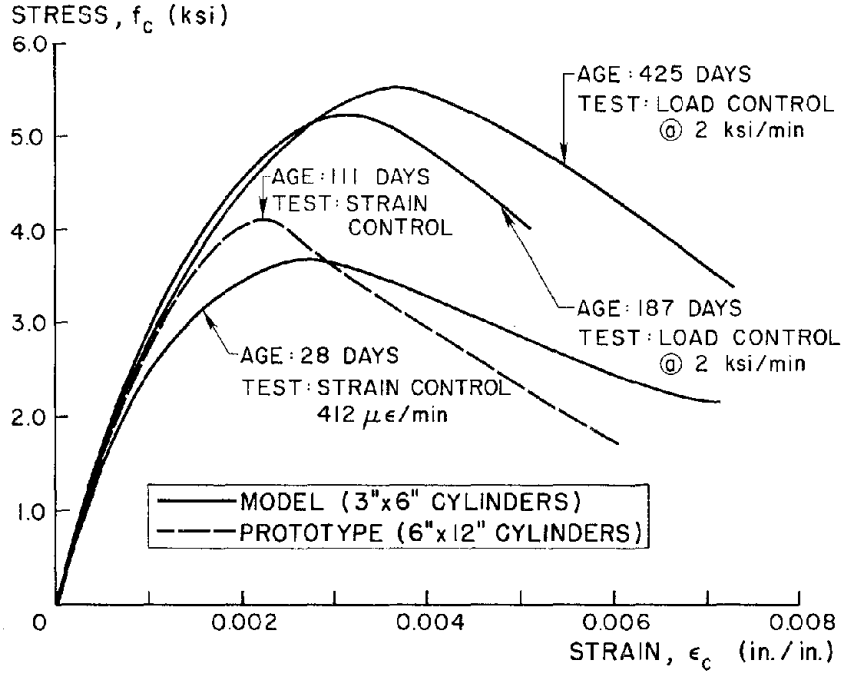

FIG. 16 STRESS-STRAIN RELATIONSHIP OF CONCRETE IN FOURTH STORY.
1 ksi = 6.9 MN/m^2 1 in. = 25.4 mm

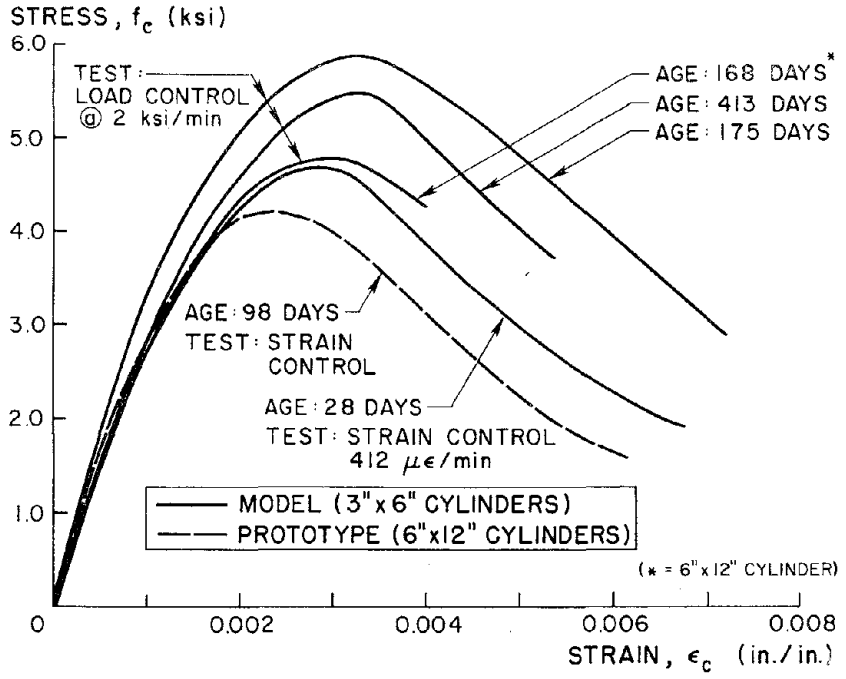

FIG. 17 STRESS-STRAIN RELATIONSHIP OF CONCRETE IN FIFTH STORY.
1ksi = 6.9 MN/m^2 1 in. = 25.4 mm

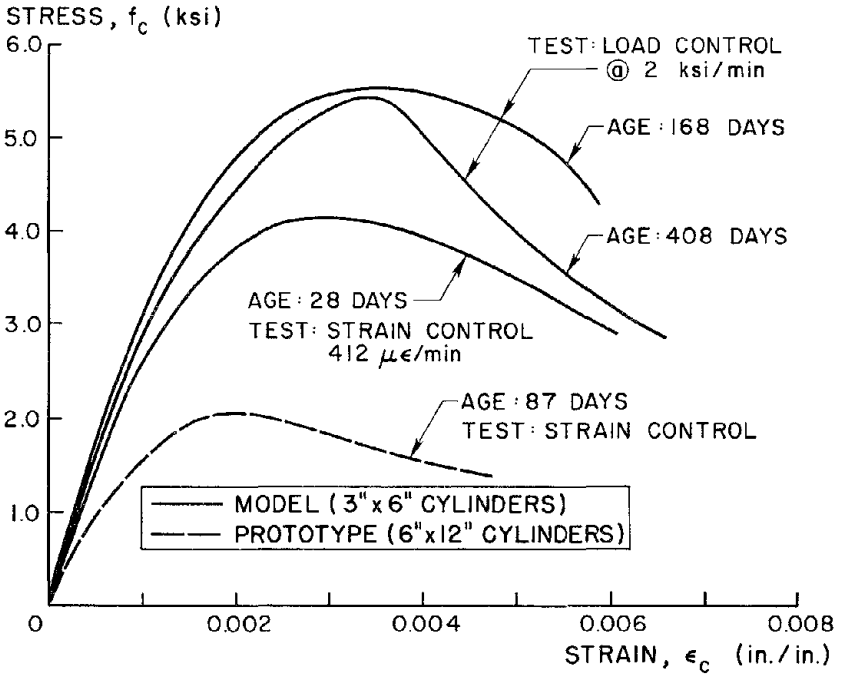

FIG. 18 STRESS-STRAIN RELATIONSHIP OF CONCRETE IN SIXTH STORY.
1ksi = 6.9 MN/m^2 1 in. = 25.4 mm

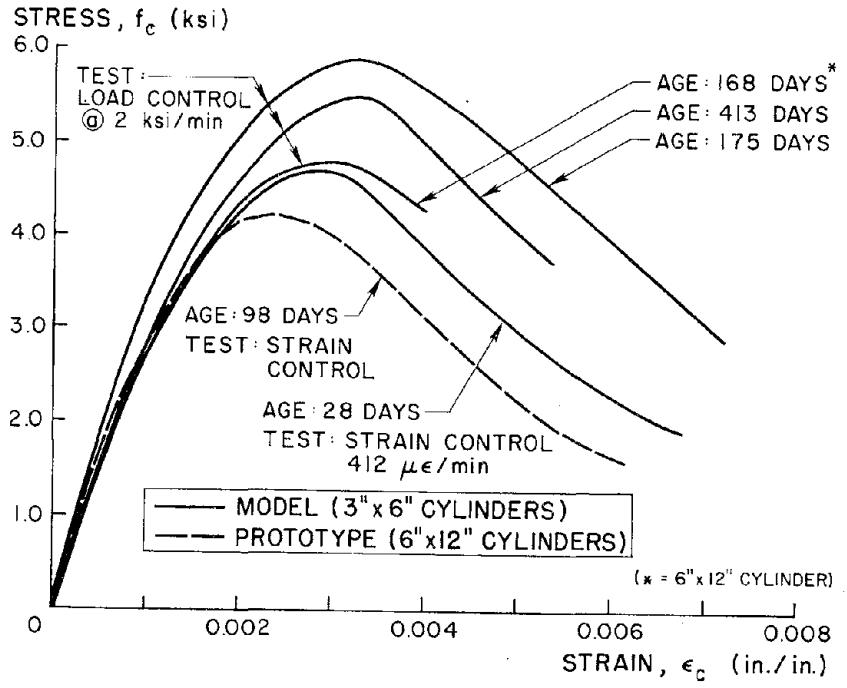

FIG. 19 STRESS-STRAIN RELATIONSHIP OF CONCRETE IN SEVENTH STORY.
1 ksi = 6.9 MN/m^2 1 in. = 25.4 mm

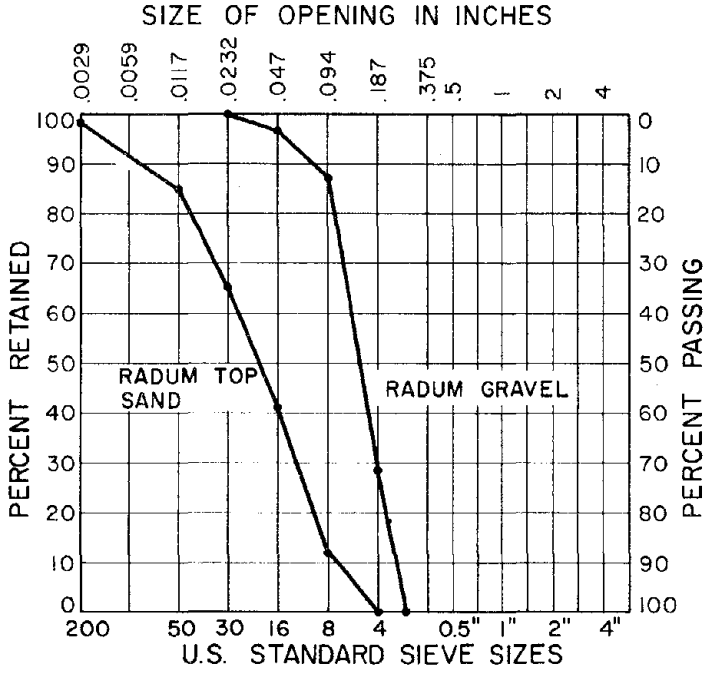

FIG. 20 GRADATION OF GRAVEL AND TOP SAND USED IN THE MICROCONCRETE.
1 in. = 25.4 mm

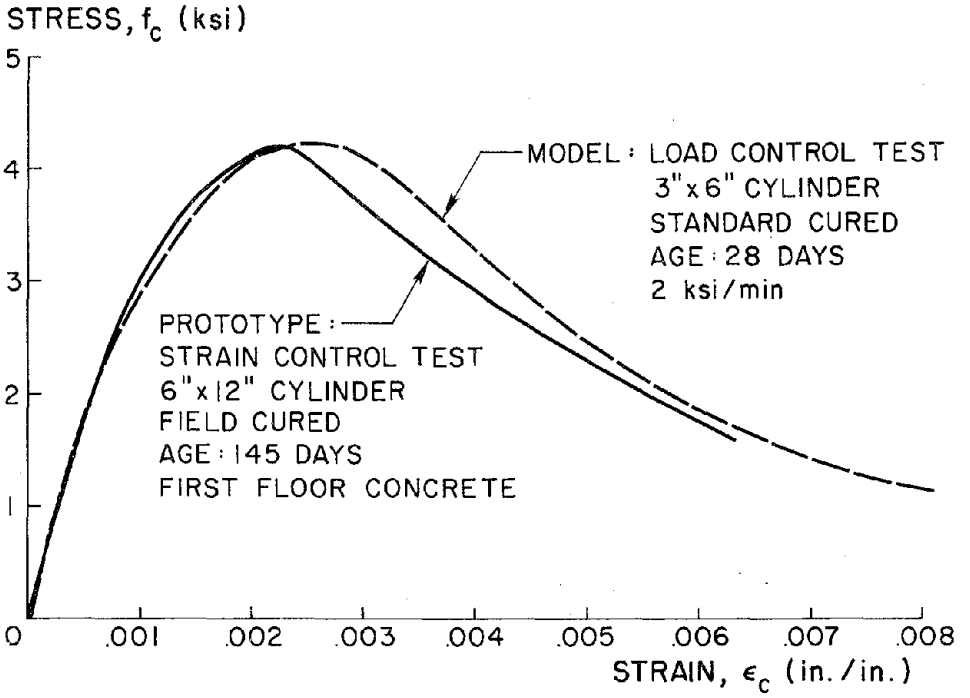

FIG. 21 STRESS-STRAIN RELATIONS OF THE PROTOTYPE AND MICRO-CONCRETE USED TO SELECT THE MICROCONCRETE MIX FOR MODEL FABRICATION. 1ksi = 6.9 MN/m^2 1 in. = 25.4 mm

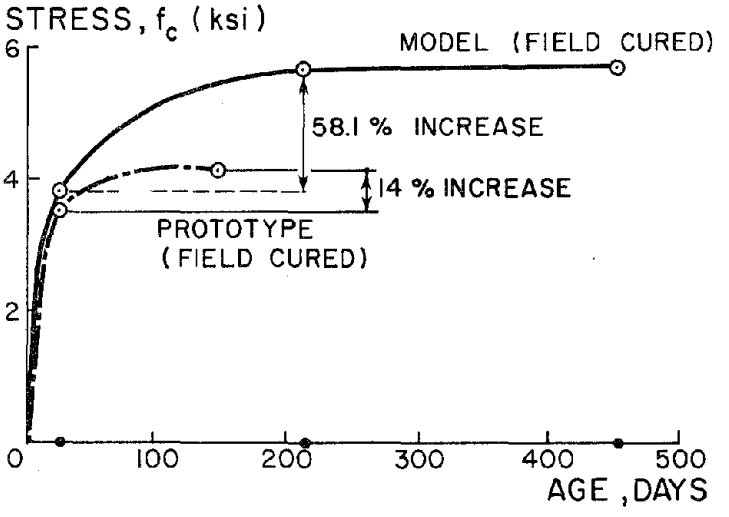

FIG. 22 VARIATION OF MAXIMUM CONCRETE STRESS WITH AGE. (FIRST FLOOR) 1ksi = 6.9 MN/m^2

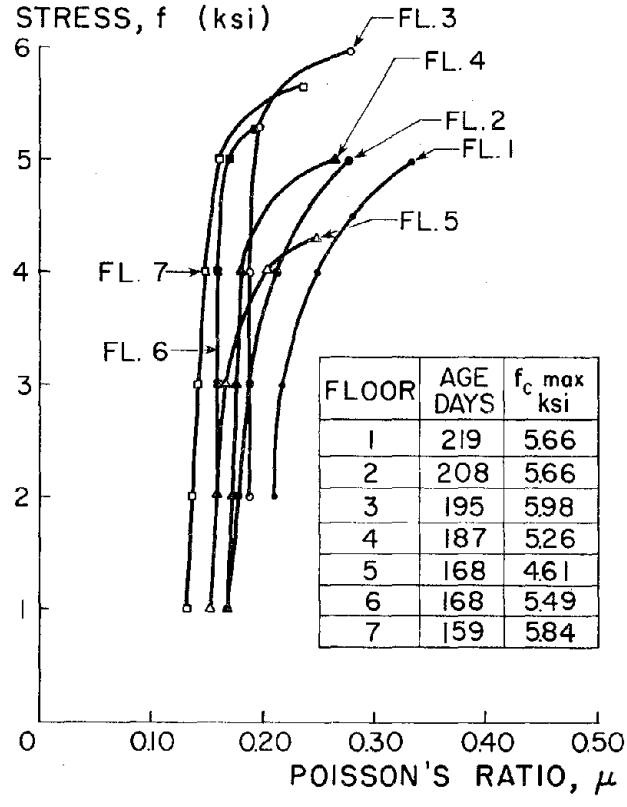

FLOOR	AGE DAYS	f_c max ksi
1	219	5.66
2	208	5.66
3	195	5.98
4	187	5.26
5	168	4.61
6	168	5.49
7	159	5.84

FIG. 23 POISSON'S RATIO OF MODEL CONCRETE.
1ksi = 6.9 MN/m^2

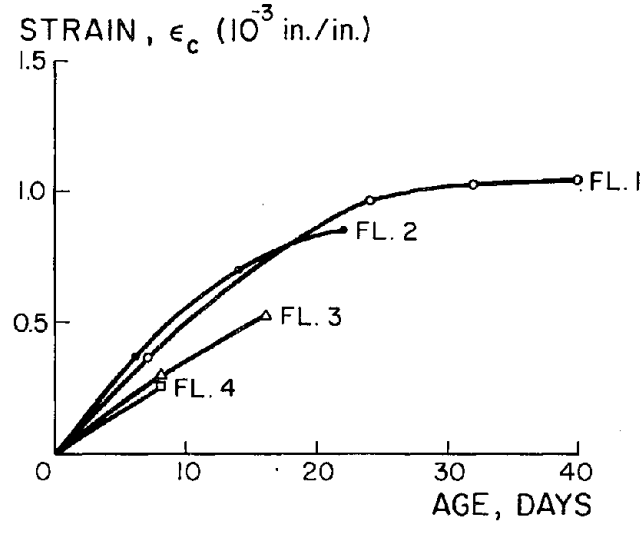

FIG. 24 SHRINKAGE STRAIN OF MODEL CONCRETE WITH AGE.
1 in. = 25.4 mm

APPENDIX A - CONVERSION FACTORS

1 ft. = 0.3048 m
1 in. = 25.4 mm = 2.54 cm
1 sq. in. = 6.451 sq. cm
1 lbf = 4.448 N
1 kip = 4.448 kN
1 psi = 6.895 kPa
1 ksi = 6.895 MPa

EARTHQUAKE ENGINEERING RESEARCH CENTER REPORTS

NOTE: Numbers in parentheses are Accession Numbers assigned by the National Technical Information Service; these are followed by a price code. Copies of the reports may be ordered from the National Technical Information Service, 5285 Port Royal Road, Springfield, Virginia, 22161. Accession Numbers should be quoted on orders for reports (PB --- ---) and remittance must accompany each order. Reports without this information were not available at time of printing. The complete list of EERC reports (from EERC 67-1) is available upon request from the Earthquake Engineering Research Center, University of California, Berkeley, 47th Street and Hoffman Boulevard, Richmond, California 94804.

UCB/EERC-77/01 "PLUSH - A Computer Program for Probabilistic Finite Element Analysis of Seismic Soil-Structure Interaction," by M.P. Romo Organista, J. Lysmer and H.B. Seed - 1977 (PB81 177 651)A05

UCB/EERC-77/02 "Soil-Structure Interaction Effects at the Humboldt Bay Power Plant in the Ferndale Earthquake of June 7, 1975," by J.E. Valera, H.B. Seed, C.F. Tsai and J. Lysmer - 1977 (PB 265 795)A04

UCB/EERC-77/03 "Influence of Sample Disturbance on Sand Response to Cyclic Loading," by K. Mori, H.B. Seed and C.K. Chan - 1977 (PB 267 352)A04

UCB/EERC-77/04 "Seismological Studies of Strong Motion Records," by J. Shoja-Taheri - 1977 (PB 269 655)A10

UCB/EERC-77/05 Unassigned

UCB/EERC-77/06 "Developing Methodologies for Evaluating the Earthquake Safety of Existing Buildings," by No. 1 - B. Bresler; No. 2 - B. Bresler, T. Okada and D. Zisling; No. 3 - T. Okada and B. Bresler; No. 4 - V.V. Bertero and B. Bresler - 1977 (PB 267 354)A08

UCB/EERC-77/07 "A Literature Survey - Transverse Strength of Masonry Walls," by Y. Omote, R.L. Mayes, S.W. Chen and R.W. Clough - 1977 (PB 277 933)A07

UCB/EERC-77/08 "DRAIN-TABS: A Computer Program for Inelastic Earthquake Response of Three Dimensional Buildings," by R. Guendelman-Israel and G.H. Powell - 1977 (PB 270 693)A07

UCB/EERC-77/09 "SUBWALL: A Special Purpose Finite Element Computer Program for Practical Elastic Analysis and Design of Structural Walls with Substructure Option," by D.Q. Le, H. Peterson and E.P. Popov - 1977 (PB 270 567)A05

UCB/EERC-77/10 "Experimental Evaluation of Seismic Design Methods for Broad Cylindrical Tanks," by D.P. Clough (PB 272 280)A13

UCB/EERC-77/11 "Earthquake Engineering Research at Berkeley - 1976," - 1977 (PB 273 507)A09

UCB/EERC-77/12 "Automated Design of Earthquake Resistant Multistory Steel Building Frames," by N.D. Walker, Jr. - 1977 (PB 276 526)A09

UCB/EERC-77/13 "Concrete Confined by Rectangular Hoops Subjected to Axial Loads," by J. Vallenas, V.V. Bertero and E.P. Popov - 1977 (PB 275 165)A06

UCB/EERC-77/14 "Seismic Strain Induced in the Ground During Earthquakes," by Y. Sugimura - 1977 (PB 284 201)A04

UCB/EERC-77/15 Unassigned

UCB/EERC-77/16 "Computer Aided Optimum Design of Ductile Reinforced Concrete Moment Resisting Frames," by S.W. Zagajeski and V.V. Bertero - 1977 (PB 280 137)A07

UCB/EERC-77/17 "Earthquake Simulation Testing of a Stepping Frame with Energy-Absorbing Devices," by J.M. Kelly and D.F. Tsztoo - 1977 (PB 273 506)A04

UCB/EERC-77/18 "Inelastic Behavior of Eccentrically Braced Steel Frames under Cyclic Loadings," by C.W. Roeder and E.P. Popov - 1977 (PB 275 526)A15

UCB/EERC-77/19 "A Simplified Procedure for Estimating Earthquake-Induced Deformations in Dams and Embankments," by F.I. Makdisi and H.B. Seed - 1977 (PB 276 820)A04

UCB/EERC-77/20 "The Performance of Earth Dams during Earthquakes," by H.B. Seed, F.I. Makdisi and P. de Alba - 1977 (PB 276 821)A04

UCB/EERC-77/21 "Dynamic Plastic Analysis Using Stress Resultant Finite Element Formulation," by P. Lukkunapvasit and J.M. Kelly - 1977 (PB 275 453)A04

UCB/EERC-77/22 "Preliminary Experimental Study of Seismic Uplift of a Steel Frame," by R.W. Clough and A.A. Huckelbridge 1977 (PB 278 769)A08

UCB/EERC-77/23 "Earthquake Simulator Tests of a Nine-Story Steel Frame with Columns Allowed to Uplift," by A.A. Huckelbridge - 1977 (PB 277 944)A09

UCB/EERC-77/24 "Nonlinear Soil-Structure Interaction of Skew Highway Bridges," by M.-C. Chen and J. Penzien - 1977 (PB 276 176)A07

UCB/EERC-77/25 "Seismic Analysis of an Offshore Structure Supported on Pile Foundations," by D.D.-N. Liou and J. Penzien 1977 (PB 283 180)A06

UCB/EERC-77/26 "Dynamic Stiffness Matrices for Homogeneous Viscoelastic Half-Planes," by G. Dasgupta and A.K. Chopra - 1977 (PB 279 654)A06

UCB/EERC-77/27 "A Practical Soft Story Earthquake Isolation System," by J.M. Kelly, J.M. Eidinger and C.J. Derham - 1977 (PB 276 814)A07

UCB/EERC-77/28 "Seismic Safety of Existing Buildings and Incentives for Hazard Mitigation in San Francisco: An Exploratory Study," by A.J. Meltsner - 1977 (PB 281 970)A05

UCB/EERC-77/29 "Dynamic Analysis of Electrohydraulic Shaking Tables," by D. Rea, S. Abedi-Hayati and Y. Takahashi 1977 (PB 282 569)A04

UCB/EERC-77/30 "An Approach for Improving Seismic - Resistant Behavior of Reinforced Concrete Interior Joints," by B. Galunic, V.V. Bertero and E.P. Popov - 1977 (PB 290 870)A06

UCB/EERC-78/01 "The Development of Energy-Absorbing Devices for Aseismic Base Isolation Systems," by J.M. Kelly and D.F. Tsztoo - 1978 (PB 284 978)A04

UCB/EERC-78/02 "Effect of Tensile Prestrain on the Cyclic Response of Structural Steel Connections, by J.G. Bouwkamp and A. Mukhopadhyay - 1978

UCB/EERC-78/03 "Experimental Results of an Earthquake Isolation System using Natural Rubber Bearings," by J.M. Eidinger and J.M. Kelly - 1978 (PB 281 686)A04

UCB/EERC-78/04 "Seismic Behavior of Tall Liquid Storage Tanks," by A. Niwa - 1978 (PB 284 017)A14

UCB/EERC-78/05 "Hysteretic Behavior of Reinforced Concrete Columns Subjected to High Axial and Cyclic Shear Forces," by S.W. Zagajeski, V.V. Bertero and J.G. Bouwkamp - 1978 (PB 283 858)A13

UCB/EERC-78/06 "Three Dimensional Inelastic Frame Elements for the ANSR-I Program," by A. Riahi, D.G. Row and G.H. Powell - 1978 (PB 295 755)A04

UCB/EERC-78/07 "Studies of Structural Response to Earthquake Ground Motion," by O.A. Lopez and A.K. Chopra - 1978 (PB 282 790)A05

UCB/EERC-78/08 "A Laboratory Study of the Fluid-Structure Interaction of Submerged Tanks and Caissons in Earthquakes," by R.C. Byrd - 1978 (PB 284 957)A08

UCB/EERC-78/09 Unassigned

UCB/EERC-78/10 "Seismic Performance of Nonstructural and Secondary Structural Elements," by I. Sakamoto - 1978 (PB81 154 593)A05

UCB/EERC-78/11 "Mathematical Modelling of Hysteresis Loops for Reinforced Concrete Columns," by S. Nakata, T. Sproul and J. Penzien - 1978 (PB 298 274)A05

UCB/EERC-78/12 "Damageability in Existing Buildings," by T. Blejwas and B. Bresler - 1978 (PB 80 166 978)A05

UCB/EERC-78/13 "Dynamic Behavior of a Pedestal Base Multistory Building," by R.M. Stephen, E.L. Wilson, J.G. Bouwkamp and M. Button - 1978 (PB 286 650)A08

UCB/EERC-78/14 "Seismic Response of Bridges - Case Studies," by R.A. Imbsen, V. Nutt and J. Penzien - 1978 (PB 286 503)A10

UCB/EERC-78/15 "A Substructure Technique for Nonlinear Static and Dynamic Analysis," by D.G. Row and G.H. Powell - 1978 (PB 288 077)A10

UCB/EERC-78/16 "Seismic Risk Studies for San Francisco and for the Greater San Francisco Bay Area," by C.S. Oliveira - 1978 (PB 81 120 115)A07

UCB/EERC-78/17 "Strength of Timber Roof Connections Subjected to Cyclic Loads," by P. Gülkan, R.L. Mayes and R.W. Clough - 1978 (HUD-000 1491)A07

UCB/EERC-78/18 "Response of K-Braced Steel Frame Models to Lateral Loads," by J.G. Bouwkamp, R.M. Stephen and E.P. Popov - 1978

UCB/EERC-78/19 "Rational Design Methods for Light Equipment in Structures Subjected to Ground Motion," by J.L. Sackman and J.M. Kelly - 1978 (PB 292 357)A04

UCB/EERC-78/20 "Testing of a Wind Restraint for Aseismic Base Isolation," by J.M. Kelly and D.E. Chitty - 1978 (PB 292 833)A03

UCB/EERC-78/21 "APOLLO - A Computer Program for the Analysis of Pore Pressure Generation and Dissipation in Horizontal Sand Layers During Cyclic or Earthquake Loading," by P.P. Martin and H.B. Seed - 1978 (PB 292 835)A04

UCB/EERC-78/22 "Optimal Design of an Earthquake Isolation System," by M.A. Bhatti, K.S. Pister and E. Polak - 1978 (PB 294 735)A06

UCB/EERC-78/23 "MASH - A Computer Program for the Non-Linear Analysis of Vertically Propagating Shear Waves in Horizontally Layered Deposits," by P.P. Martin and H.B. Seed - 1978 (PB 293 101)A05

UCB/EERC-78/24 "Investigation of the Elastic Characteristics of a Three Story Steel Frame Using System Identification," by I. Kaya and H.D. McNiven - 1978 (PB 296 225)A06

UCB/EERC-78/25 "Investigation of the Nonlinear Characteristics of a Three-Story Steel Frame Using System Identification," by I. Kaya and H.D. McNiven - 1978 (PB 301 363)A05

UCB/EERC-78/26 "Studies of Strong Ground Motion in Taiwan," by Y.M. Hsiung, B.A. Bolt and J. Penzien - 1978 (PB 298 436)A06

UCB/EERC-78/27 "Cyclic Loading Tests of Masonry Single Piers: Volume 1 - Height to Width Ratio of 2," by P.A. Hidalgo, R.L. Mayes, H.D. McNiven and R.W. Clough - 1978 (PB 296 211)A07

UCB/EERC-78/28 "Cyclic Loading Tests of Masonry Single Piers: Volume 2 - Height to Width Ratio of 1," by S.-W.J. Chen, P.A. Hidalgo, R.L. Mayes, R.W. Clough and H.D. McNiven - 1978 (PB 296 212)A09

UCB/EERC-78/29 "Analytical Procedures in Soil Dynamics," by J. Lysmer - 1978 (PB 298 445)A06

UCB/EERC-79/01 "Hysteretic Behavior of Lightweight Reinforced Concrete Beam-Column Subassemblages," by B. Forzani, E.P. Popov and V.V. Bertero - April 1979(PB 298 267)A06

UCB/EERC-79/02 "The Development of a Mathematical Model to Predict the Flexural Response of Reinforced Concrete Beams to Cyclic Loads, Using System Identification," by J. Stanton & H. McNiven - Jan. 1979(PB 295 875)A10

UCB/EERC-79/03 "Linear and Nonlinear Earthquake Response of Simple Torsionally Coupled Systems," by C.L. Kan and A.K. Chopra - Feb. 1979(PB 298 262)A06

UCB/EERC-79/04 "A Mathematical Model of Masonry for Predicting its Linear Seismic Response Characteristics," by Y. Mengi and H.D. McNiven - Feb. 1979(PB 298 266)A06

UCB/EERC-79/05 "Mechanical Behavior of Lightweight Concrete Confined by Different Types of Lateral Reinforcement," by M.A. Manrique, V.V. Bertero and E.P. Popov - May 1979(PB 301 114)A06

UCB/EERC-79/06 "Static Tilt Tests of a Tall Cylindrical Liquid Storage Tank," by R.W. Clough and A. Niwa - Feb. 1979 (PB 301 167)A06

UCB/EERC-79/07 "The Design of Steel Energy Absorbing Restrainers and Their Incorporation into Nuclear Power Plants for Enhanced Safety: Volume 1 - Summary Report," by P.N. Spencer, V.F. Zackay, and E.R. Parker - Feb. 1979(UCB/EERC-79/07)A09

UCB/EERC-79/08 "The Design of Steel Energy Absorbing Restrainers and Their Incorporation into Nuclear Power Plants for Enhanced Safety: Volume 2 - The Development of Analyses for Reactor System Piping,""Simple Systems" by M.C. Lee, J. Penzien, A.K. Chopra and K, Suzuki "Complex Systems" by G.H. Powell, E.L. Wilson, R.W. Clough and D.G. Row - Feb. 1979(UCB/EERC-79/08)A10

UCB/EERC-79/09 "The Design of Steel Energy Absorbing Restrainers and Their Incorporation into Nuclear Power Plants for Enhanced Safety: Volume 3 - Evaluation of Commercial Steels," by W.S. Owen, R.M.N. Pelloux, R.O. Ritchie, M. Faral, T. Ohhashi, J. Toplosky, S.J. Hartman, V.F. Zackay and E.R. Parker - Feb. 1979(UCB/EERC-79/09)A04

UCB/EERC-79/10 "The Design of Steel Energy Absorbing Restrainers and Their Incorporation into Nuclear Power Plants for Enhanced Safety: Volume 4 - A Review of Energy-Absorbing Devices," by J.M. Kelly and M.S. Skinner - Feb. 1979(UCB/EERC-79/10)A04

UCB/EERC-79/11 "Conservatism In Summation Rules for Closely Spaced Modes," by J.M. Kelly and J.L. Sackman - May 1979(PB 301 328)A03

UCB/EERC-79/12 "Cyclic Loading Tests of Masonry Single Piers; Volume 3 - Height to Width Ratio of 0.5," by P.A. Hidalgo, R.L. Mayes, H.D. McNiven and R.W. Clough - May 1979(PB 301 321)A08

UCB/EERC-79/13 "Cyclic Behavior of Dense Course-Grained Materials in Relation to the Seismic Stability of Dams," by N.G. Banerjee, H.B. Seed and C.K. Chan - June 1979(PB 301 373)A13

UCB/EERC-79/14 "Seismic Behavior of Reinforced Concrete Interior Beam-Column Subassemblages," by S. Viwathanatepa, E.P. Popov and V.V. Bertero - June 1979(PB 301 326)A10

UCB/EERC-79/15 "Optimal Design of Localized Nonlinear Systems with Dual Performance Criteria Under Earthquake Excitations," by M.A. Bhatti - July 1979(PB 80 167 109)A06

UCB/EERC-79/16 "OPTDYN - A General Purpose Optimization Program for Problems with or without Dynamic Constraints," by M.A. Bhatti, E. Polak and K.S. Pister - July 1979(PB 80 167 091)A05

UCB/EERC-79/17 "ANSR-II, Analysis of Nonlinear Structural Response, Users Manual," by D.P. Mondkar and G.H. Powell July 1979(PB 80 113 301)A05

UCB/EERC-79/18 "Soil Structure Interaction in Different Seismic Environments," A. Gomez-Masso, J. Lysmer, J.-C. Chen and H.B. Seed - August 1979(PB 80 101 520)A04

UCB/EERC-79/19 "ARMA Models for Earthquake Ground Motions," by M.K. Chang, J.W. Kwiatkowski, R.F. Nau, R.M. Oliver and K.S. Pister - July 1979(PB 301 166)A05

UCB/EERC-79/20 "Hysteretic Behavior of Reinforced Concrete Structural Walls," by J.M. Vallenas, V.V. Bertero and E.P. Popov - August 1979(PB 80 165 905)A12

UCB/EERC-79/21 "Studies on High-Frequency Vibrations of Buildings - 1: The Column Effect," by J. Lubliner - August 1979 (PB 80 158 553)A03

UCB/EERC-79/22 "Effects of Generalized Loadings on Bond Reinforcing Bars Embedded in Confined Concrete Blocks," by S. Viwathanatepa, E.P. Popov and V.V. Bertero - August 1979(PB 81 124 018)A14

UCB/EERC-79/23 "Shaking Table Study of Single-Story Masonry Houses, Volume 1: Test Structures 1 and 2," by P. Gülkan, R.L. Mayes and R.W. Clough - Sept. 1979 (HUD-000 1763)A12

UCB/EERC-79/24 "Shaking Table Study of Single-Story Masonry Houses, Volume 2: Test Structures 3 and 4," by P. Gülkan, R.L. Mayes and R.W. Clough - Sept. 1979 (HUD-000 1836)A12

UCB/EERC-79/25 "Shaking Table Study of Single-Story Masonry Houses, Volume 3: Summary, Conclusions and Recommendations," by R.W. Clough, R.L. Mayes and P. Gülkan - Sept. 1979 (HUD-000 1837)A06

UCB/EERC-79/26 "Recommendations for a U.S.-Japan Cooperative Research Program Utilizing Large-Scale Testing Facilities," by U.S.-Japan Planning Group - Sept. 1979(PB 301 407)A06

UCB/EERC-79/27 "Earthquake-Induced Liquefaction Near Lake Amatitlan, Guatemala," by H.B. Seed, I. Arango, C.K. Chan, A. Gomez-Masso and R. Grant de Ascoli - Sept. 1979(NUREG-CR1341)A03

UCB/EERC-79/28 "Infill Panels: Their Influence on Seismic Response of Buildings," by J.W. Axley and V.V. Bertero Sept. 1979(PB 80 163 371)A10

UCB/EERC-79/29 "3D Truss Bar Element (Type 1) for the ANSR-II Program," by D.P. Mondkar and G.H. Powell - Nov. 1979 (PB 80 169 709)A02

UCB/EERC-79/30 "2D Beam-Column Element (Type 5 - Parallel Element Theory) for the ANSR-II Program," by D.G. Row, G.H. Powell and D.P. Mondkar - Dec. 1979(PB 80 167 224)A03

UCB/EERC-79/31 "3D Beam-Column Element (Type 2 - Parallel Element Theory) for the ANSR-II Program," by A. Riahi, G.H. Powell and D.P. Mondkar - Dec. 1979(PB 80 167 216)A03

UCB/EERC-79/32 "On Response of Structures to Stationary Excitation," by A. Der Kiureghian - Dec. 1979(PB 80166 929)A03

UCB/EERC-79/33 "Undisturbed Sampling and Cyclic Load Testing of Sands," by S. Singh, H.B. Seed and C.K. Chan Dec. 1979(ADA 087 298)A07

UCB/EERC-79/34 "Interaction Effects of Simultaneous Torsional and Compressional Cyclic Loading of Sand," by P.M. Griffin and W.N. Houston - Dec. 1979(ADA 092 352)A15

UCB/EERC-80/01 "Earthquake Response of Concrete Gravity Dams Including Hydrodynamic and Foundation Interaction Effects," by A.K. Chopra, P. Chakrabarti and S. Gupta - Jan. 1980(AD-A087297)A10

UCB/EERC-80/02 "Rocking Response of Rigid Blocks to Earthquakes," by C.S. Yim, A.K. Chopra and J. Penzien - Jan. 1980 (PB80 166 002)A04

UCB/EERC-80/03 "Optimum Inelastic Design of Seismic-Resistant Reinforced Concrete Frame Structures," by S.W. Zagajeski and V.V. Bertero - Jan. 1980(PB80 164 635)A06

UCB/EERC-80/04 "Effects of Amount and Arrangement of Wall-Panel Reinforcement on Hysteretic Behavior of Reinforced Concrete Walls," by R. Iliya and V.V. Bertero - Feb. 1980(PB81 122 525)A09

UCB/EERC-80/05 "Shaking Table Research on Concrete Dam Models," by A. Niwa and R.W. Clough - Sept. 1980(PB81 122 368)A06

UCB/EERC-80/06 "The Design of Steel Energy-Absorbing Restrainers and their Incorporation into Nuclear Power Plants for Enhanced Safety (Vol 1A): Piping with Energy Absorbing Restrainers: Parameter Study on Small Systems," by G.H. Powell, C. Oughourlian and J. Simons - June 1980

UCB/EERC-80/07 "Inelastic Torsional Response of Structures Subjected to Earthquake Ground Motions," by Y. Yamazaki April 1980(PB81 122 327)A08

UCB/EERC-80/08 "Study of X-Braced Steel Frame Structures Under Earthquake Simulation," by Y. Ghanaat - April 1980 (PB81 122 335)A11

UCB/EERC-80/09 "Hybrid Modelling of Soil-Structure Interaction," by S. Gupta, T.W. Lin, J. Penzien and C.S. Yeh May 1980(PB81 122 319)A07

UCB/EERC-80/10 "General Applicability of a Nonlinear Model of a One Story Steel Frame," by B.I. Sveinsson and H.D. McNiven - May 1980(PB81 124 877)A06

UCB/EERC-80/11 "A Green-Function Method for Wave Interaction with a Submerged Body," by W. Kioka - April 1980 (PB81 122 269)A07

UCB/EERC-80/12 "Hydrodynamic Pressure and Added Mass for Axisymmetric Bodies," by F. Nilrat - May 1980(PB81 122 343)A08

UCB/EERC-80/13 "Treatment of Non-Linear Drag Forces Acting on Offshore Platforms," by B.V. Dao and J. Penzien May 1980(PB81 153 413)A07

UCB/EERC-80/14 "2D Plane/Axisymmetric Solid Element (Type 3 - Elastic or Elastic-Perfectly Plastic) for the ANSR-II Program," by D.P. Mondkar and G.H. Powell - July 1980(PB81 122 350)A03

UCB/EERC-80/15 "A Response Spectrum Method for Random Vibrations," by A. Der Kiureghian - June 1980(PB81 122 301)A03

UCB/EERC-80/16 "Cyclic Inelastic Buckling of Tubular Steel Braces," by V.A. Zayas, E.P. Popov and S.A. Mahin June 1980(PB81 124 885)A10

UCB/EERC-80/17 "Dynamic Response of Simple Arch Dams Including Hydrodynamic Interaction," by C.S. Porter and A.K. Chopra - July 1980(PB81 124 000)A13

UCB/EERC-80/18 "Experimental Testing of a Friction Damped Aseismic Base Isolation System with Fail-Safe Characteristics," by J.M. Kelly, K.E. Beucke and M.S. Skinner - July 1980(PB81 148 595)A04

UCB/EERC-80/19 "The Design of Steel Energy-Absorbing Restrainers and their Incorporation into Nuclear Power Plants for Enhanced Safety (Vol 1B): Stochastic Seismic Analyses of Nuclear Power Plant Structures and Piping Systems Subjected to Multiple Support Excitations," by M.C. Lee and J. Penzien - June 1980

UCB/EERC-80/20 "The Design of Steel Energy-Absorbing Restrainers and their Incorporation into Nuclear Power Plants for Enhanced Safety (Vol 1C): Numerical Method for Dynamic Substructure Analysis," by J.M. Dickens and E.L. Wilson - June 1980

UCB/EERC-80/21 "The Design of Steel Energy-Absorbing Restrainers and their Incorporation into Nuclear Power Plants for Enhanced Safety (Vol 2): Development and Testing of Restraints for Nuclear Piping Systems," by J.M. Kelly and M.S. Skinner - June 1980

UCB/EERC-80/22 "3D Solid Element (Type 4-Elastic or Elastic-Perfectly-Plastic) for the ANSR-II Program," by D.P. Mondkar and G.H. Powell - July 1980(PB81 123 242)A03

UCB/EERC-80/23 "Gap-Friction Element (Type 5) for the ANSR-II Program," by D.P. Mondkar and G.H. Powell - July 1980 (PB81 122 285)A03

UCB/EERC-80/24 "U-Bar Restraint Element (Type 11) for the ANSR-II Program," by C. Oughourlian and G.H. Powell July 1980(PB81 122 293)A03

UCB/EERC-80/25 "Testing of a Natural Rubber Base Isolation System by an Explosively Simulated Earthquake," by J.M. Kelly - August 1980(PB81 201 360)A04

UCB/EERC-80/26 "Input Identification from Structural Vibrational Response," by Y. Hu - August 1980(PB81 152 308)A05

UCB/EERC-80/27 "Cyclic Inelastic Behavior of Steel Offshore Structures," by V.A. Zayas, S.A. Mahin and E.P. Popov August 1980(PB81 196 180)A15

UCB/EERC-80/28 "Shaking Table Testing of a Reinforced Concrete Frame with Biaxial Response," by M.G. Oliva October 1980(PB81 154 304)A10

UCB/EERC-80/29 "Dynamic Properties of a Twelve-Story Prefabricated Panel Building," by J.G. Bouwkamp, J.P. Kollegger and R.M. Stephen - October 1980(PB82 117 128)A06

UCB/EERC-80/30 "Dynamic Properties of an Eight-Story Prefabricated Panel Building," by J.G. Bouwkamp, J.P. Kollegger and R.M. Stephen - October 1980(PB81 200 313)A05

UCB/EERC-80/31 "Predictive Dynamic Response of Panel Type Structures Under Earthquakes," by J.P. Kollegger and J.G. Bouwkamp - October 1980(PB81 152 316)A04

UCB/EERC-80/32 "The Design of Steel Energy-Absorbing Restrainers and their Incorporation into Nuclear Power Plants for Enhanced Safety (Vol 3): Testing of Commercial Steels in Low-Cycle Torsional Fatigue," by P. Spencer, E.R. Parker, E. Jongewaard and M. Drory

UCB/EERC-80/33 "The Design of Steel Energy-Absorbing Restrainers and their Incorporation into Nuclear Power Plants for Enhanced Safety (Vol 4): Shaking Table Tests of Piping Systems with Energy-Absorbing Restrainers," by S.F. Stiemer and W.G. Godden - Sept. 1980

UCB/EERC-80/34 "The Design of Steel Energy-Absorbing Restrainers and their Incorporation into Nuclear Power Plants for Enhanced Safety (Vol 5): Summary Report," by P. Spencer

UCB/EERC-80/35 "Experimental Testing of an Energy-Absorbing Base Isolation System," by J.M. Kelly, M.S. Skinner and K.E. Beucke - October 1980(PB81 154 072)A04

UCB/EERC-80/36 "Simulating and Analyzing Artificial Non-Stationary Earthquake Ground Motions," by R.F. Nau, R.M. Oliver and K.S. Pister - October 1980(PB81 153 397)A04

UCB/EERC-80/37 "Earthquake Engineering at Berkeley - 1980," - Sept. 1980(PB81 205 874)A09

UCB/EERC-80/38 "Inelastic Seismic Analysis of Large Panel Buildings," by V. Schricker and G.H. Powell - Sept. 1980 (PB81 154 338)A13

UCB/EERC-80/39 "Dynamic Response of Embankment, Concrete-Gravity and Arch Dams Including Hydrodynamic Interaction," by J.F. Hall and A.K. Chopra - October 1980(PB81 152 324)A11

UCB/EERC-80/40 "Inelastic Buckling of Steel Struts Under Cyclic Load Reversal," by R.G. Black, W.A. Wenger and E.P. Popov - October 1980(PB81 154 312)A08

UCB/EERC-80/41 "Influence of Site Characteristics on Building Damage During the October 3, 1974 Lima Earthquake," by P. Repetto, I. Arango and H.B. Seed - Sept. 1980(PB81 161 739)A05

UCB/EERC-80/42 "Evaluation of a Shaking Table Test Program on Response Behavior of a Two Story Reinforced Concrete Frame," by J.M. Blondet, R.W. Clough and S.A. Mahin

UCB/EERC-80/43 "Modelling of Soil-Structure Interaction by Finite and Infinite Elements," by F. Medina - December 1980(PB81 229 270)A04

UCB/EERC-81/01 "Control of Seismic Response of Piping Systems and Other Structures by Base Isolation," edited by J.M. Kelly - January 1981 (PB81 200 735)A05

UCB/EERC-81/02 "OPTNSR - An Interactive Software System for Optimal Design of Statically and Dynamically Loaded Structures with Nonlinear Response," by M.A. Bhatti, V. Ciampi and K.S. Pister - January 1981 (PB81 218 851)A09

UCB/EERC-81/03 "Analysis of Local Variations in Free Field Seismic Ground Motions," by J.-C. Chen, J. Lysmer and H.B. Seed - January 1981 (AD-A099508)A13

UCB/EERC-81/04 'Inelastic Structural Modeling of Braced Offshore Platforms for Seismic Loading," by V.A. Zayas, P.-S.B. Shing, S.A. Mahin and E.P. Popov - January 1981(PB82 138 777)A07

UCB/EERC-81/05 "Dynamic Response of Light Equipment in Structures," by A. Der Kiureghian, J.L. Sackman and B. Nour-Omid - April 1981 (PB81 218 497)A04

UCB/EERC-81/06 "Preliminary Experimental Investigation of a Broad Base Liquid Storage Tank," by J.G. Bouwkamp, J.P. Kollegger and R.M. Stephen - May 1981(PB82 140 385)A03

UCB/EERC-81/07 "The Seismic Resistant Design of Reinforced Concrete Coupled Structural Walls," by A.E. Aktan and V.V. Bertero - June 1981(PB82 113 358)A11

UCB/EERC-81/08 "The Undrained Shearing Resistance of Cohesive Soils at Large Deformations," by M.R. Pyles and H.B. Seed - August 1981

UCB/EERC-81/09 "Experimental Behavior of a Spatial Piping System with Steel Energy Absorbers Subjected to a Simulated Differential Seismic Input," by S.F. Stiemer, W.G. Godden and J.M. Kelly - July 1981

UCB/EERC-81/10 "Evaluation of Seismic Design Provisions for Masonry in the United States," by B.I. Sveinsson, R.L. Mayes and H.D. McNiven - August 1981 (PB82 166 075)A08

UCB/EERC-81/11 "Two-Dimensional Hybrid Modelling of Soil-Structure Interaction," by T.-J. Tzong, S. Gupta and J. Penzien - August 1981(PB82 142 118)A04

UCB/EERC-81/12 "Studies on Effects of Infills in Seismic Resistant R/C Construction," by S. Brokken and V.V. Bertero - September 1981 (PB82 166 190)A09

UCB/EERC-81/13 "Linear Models to Predict the Nonlinear Seismic Behavior of a One-Story Steel Frame," by H. Valdimarsson, A.H. Shah and H.D. McNiven - September 1981(PB82 138 793)A07

UCB/EERC-81/14 "TLUSH: A Computer Program for the Three-Dimensional Dynamic Analysis of Earth Dams," by T. Kagawa, L.H. Mejia, H.B. Seed and J. Lysmer - September 1981(PB82 139 940)A06

UCB/EERC-81/15 "Three Dimensional Dynamic Response Analysis of Earth Dams," by L.H. Mejia and H.B. Seed - September 1981 (PB82 137 274)A12

UCB/EERC-81/16 "Experimental Study of Lead and Elastomeric Dampers for Base Isolation Systems," by J.M. Kelly and S.B. Hodder - October 1981 (PB82 166 182)A05

UCB/EERC-81/17 "The Influence of Base Isolation on the Seismic Response of Light Secondary Equipment," by J.M. Kelly - April 1981 (PB82 255 266)A04

UCB/EERC-81/18 "Studies on Evaluation of Shaking Table Response Analysis Procedures," by J. Marcial Blondet - November 1981 (PB82 197 278)A10

UCB/EERC-81/19 "DELIGHT.STRUCT: A Computer-Aided Design Environment for Structural Engineering," by R.J. Balling, K.S. Pister and E. Polak - December 1981 (PB82 218 496)A07

UCB/EERC-81/20 "Optimal Design of Seismic-Resistant Planar Steel Frames," by R.J. Balling, V. Ciampi, K.S. Pister and E. Polak - December 1981 (PB82 220 179)A07

UCB/EERC-82/01 "Dynamic Behavior of Ground for Seismic Analysis of Lifeline Systems," by T. Sato and A. Der Kiureghian - January 1982 (PB82 218 926)A05

UCB/EERC-82/02 "Shaking Table Tests of a Tubular Steel Frame Model," by Y. Ghanaat and R. W. Clough - January 1982 (PB82 220 161)A07

UCB/EERC-82/03 "Behavior of a Piping System under Seismic Excitation: Experimental Investigations of a Spatial Piping System supported by Mechanical Shock Arrestors and Steel Energy Absorbing Devices under Seismic Excitation," by S. Schneider, H.-M. Lee and W. G. Godden - May 1982 (PB83 172 544)A09

UCB/EERC-82/04 "New Approaches for the Dynamic Analysis of Large Structural Systems," by E. L. Wilson - June 1982 (PB83 148 080)A05

UCB/EERC-82/05 "Model Study of Effects of Damage on the Vibration Properties of Steel Offshore Platforms," by F. Shahrivar and J. G. Bouwkamp - June 1982 (PB83 148 742)A10

UCB/EERC-82/06 "States of the Art and Practice in the Optimum Seismic Design and Analytical Response Prediction of R/C Frame-Wall Structures," by A. E. Aktan and V. V. Bertero - July 1982 (PB83 147 736)A05

UCB/EERC-82/07 "Further Study of the Earthquake Response of a Broad Cylindrical Liquid-Storage Tank Model," by G. C. Manos and R. W. Clough - July 1982 (PB83 147 744)A11

UCB/EERC-82/08 "An Evaluation of the Design and Analytical Seismic Response of a Seven Story Reinforced Concrete Frame - Wall Structure," by F. A. Charney and V. V. Bertero - July 1982(PB83 157 628)A09

UCB/EERC-82/09 "Fluid-Structure Interactions: Added Mass Computations for Incompressible Fluid," by J. S.-H. Kuo - August 1982 (PB83 156 281)A07

UCB/EERC-82/10 "Joint-Opening Nonlinear Mechanism: Interface Smeared Crack Model," by J. S.-H. Kuo - August 1982 (PB83 149 195)A05

UCB/EERC-82/11 "Dynamic Response Analysis of Techi Dam," by R. W. Clough, R. M. Stephen and J. S.-H. Kuo - August 1982 (PB83 147 496)A06

UCB/EERC-82/12 "Prediction of the Seismic Responses of R/C Frame-Coupled Wall Structures," by A. E. Aktan, V. V. Bertero and M. Piazza - August 1982 (PB83 149 203)A09

UCB/EERC-82/13 "Preliminary Report on the SMART 1 Strong Motion Array in Taiwan," by B. A. Bolt, C. H. Loh, J. Penzien, Y. B. Tsai and Y. T. Yeh - August 1982 (PB83 159 400)A10

UCB/EERC-82/14 "Shaking-Table Studies of an Eccentrically X-Braced Steel Structure," by M. S. Yang - September 1982

UCB/EERC-82/15 "The Performance of Stairways in Earthquakes," by C. Roha, J. W. Axley and V. V. Bertero - September 1982 (PB83 157 693)A07

UCB/EERC-82/16 "The Behavior of Submerged Multiple Bodies in Earthquakes," by W.-G. Liao - Sept. 1982 (PB83 158 709)A07

UCB/EERC-82/17 "Effects of Concrete Types and Loading Conditions on Local Bond-Slip Relationships," by A. D. Cowell, E. P. Popov and V. V. Bertero - September 1982 (PB83 153 577)A04

UCB/EERC-82/18 "Mechanical Behavior of Shear Wall Vertical Boundary Members: An Experimental Investigation," by M. T. Wagner and V. V. Bertero - October 1982 (PB83 159 764)A05

UCB/EERC-82/19 "Experimental Studies of Multi-support Seismic Loading on Piping Systems," by J. M. Kelly and A. D. Cowell - November 1982

UCB/EERC-82/20 "Generalized Plastic Hinge Concepts for 3D Beam-Column Elements," by P. F.-S. Chen and G. H. Powell - November 1982

UCB/EERC-82/21 "ANSR-III: General Purpose Computer Program for Nonlinear Structural Analysis," by C. V. Oughourlian and G. H. Powell - November 1982

UCB/EERC-82/22 "Solution Strategies for Statically Loaded Nonlinear Structures," by J. W. Simons and G. H. Powell - November 1982

UCB/EERC-82/23 "Analytical Model of Deformed Bar Anchorages under Generalized Excitations," by V. Ciampi, R. Eligehausen, V. V. Bertero and E. P. Popov - November 1982 (PB83 169 532)A06

UCB/EERC-82/24 "A Mathematical Model for the Response of Masonry Walls to Dynamic Excitations," by H. Sucuoğlu, Y. Mengi and H. D. McNiven - November 1982 (PB83 169 011)A07

UCB/EERC-82/25 "Earthquake Response Considerations of Broad Liquid Storage Tanks," by F. J. Cambra - November 1982

UCB/EERC-82/26 "Computational Models for Cyclic Plasticity, Rate Dependence and Creep," by B. Mosaddad and G. H. Powell - November 1982

UCB/EERC-82/27 "Inelastic Analysis of Piping and Tubular Structures," by M. Mahasuverachai and G. H. Powell - November 1982

UCB/EERC-83/01 "The Economic Feasibility of Seismic Rehabilitation of Buildings by Base Isolation," by J. M. Kelly - January 1983

UCB/EERC-83/02 "Seismic Moment Connections for Moment-Resisting Steel Frames," by E. P. Popov - January 1983

UCB/EERC-83/03 "Design of Links and Beam-to-Column Connections for Eccentrically Braced Steel Frames," by E. P. Popov and J. O. Malley - January 1983

UCB/EERC-83/04 "Numerical Techniques for the Evaluation of Soil-Structure Interaction Effects in the Time Domain," by E. Bayo and E. L. Wilson - February 1983

UCB/EERC-83/05 "A Transducer for Measuring the Internal Forces in the Columns of a Frame-Wall Reinforced Concrete Structure," by R. Sause and V. V. Bertero - May 1983

UCB/EERC-83/06 "Dynamic Interactions between Floating Ice and Offshore Structures," by P. Croteau - May 1983

UCB/EERC-83/07 "Dynamic Analysis of Multiply Tuned and Arbitrarily Supported Secondary Systems," by T. Igusa and A. Der Kiureghian - June 1983

UCB/EERC-83/08 "A Laboratory Study of Submerged Multi-body Systems in Earthquakes," by G. R. Ansari - June 1983

UCB/EERC-83/09 "Effects of Transient Foundation Uplift on Earthquake Response of Structures," by C.-S. Yim and A. K. Chopra - June 1983

UCB/EERC-83/10 "Optimal Design of Friction-Braced Frames under Seismic Loading," by M. A. Austin and K. S. Pister - June 1983

UCB/EERC-83/11 "Shaking Table Study of Single-Story Masonry Houses: Dynamic Performance under Three Component Seismic Input and Recommendations," by G. C. Manos, R. W. Clough and R. L. Mayes - June 1983

UCB/EERC-83/12 "Experimental Error Propagation in Pseudodynamic Testing," by P. B. Shing and S. A. Mahin - June 1983

UCB/EERC-83/13 "Experimental and Analytical Predictions of the Mechanical Characteristics of a 1/5-scale Model of a 7-story R/C Frame-Wall Building Structure," by A. E. Aktan, V. V. Bertero, A. A. Chowdhury and T. Nagashima - August 1983

UCB/EERC-83/14 "Shaking Table Tests of Large-Panel Precast Concrete Building System Assemblages," by M. G. Oliva and R. W. Clough - August 1983

UCB/EERC-83/15 "Seismic Behavior of Active Beam Links in Eccentrically Braced Frames," by K. D. Hjelmstad and E. P. Popov - July 1983

UCB/EERC-83/16 "System Identification of Structures with Joint Rotation," by J. S. Dimsdale and H. D. McNiven - July 1983

UCB/EERC-83/17 "Construction of Inelastic Response Spectra for Single-Degree-of-Freedom Systems," by S. Mahin and J. Lin - July 1983

UCB/EERC-83/18 "Interactive Computer Analysis Methods for Predicting the Inelastic Cyclic Behavior of Sections," by S. Kaba and S. Mahin - July 1983

UCB/EERC-83/19 "Effects of Bond Deterioration on Hysteretic Behavior of Reinforced Concrete Joints," by F. C. Filippou, E. P. Popov and V. V. Bertero - August 1983

UCB/EERC-83/20 "Analytical and Experimental Correlation of Large-Panel Precast Building System Performance," by M. G. Oliva, R. W. Clough, M. Velkov, P. Gavrilovic and J. Petrovski - November 1983

UCB/EERC-83/21 "MECHANICAL CHARACTERISTICS OF MATERIALS USED IN A 1/5 SCALE MODEL OF A 7-STORY REINFORCED CONCRETE TEST STRUCTURE," by V. V. BERTERO, A. E. AKTAN, H. G. HARRIS AND A. A. CHOWDHURY - October 1983